JOURNAL OF CHEMICAL & ENGINEERING DATA

ARTICLE

pubs.acs.org/jced

Simultaneous Viscosity−Density Measurements on Ethane and Propane over a Wide Range of Temperature and Pressure Including the Near-Critical Region

Daniel Seibt,[†] Karsten Voß,[‡] Sebastian Herrmann,[‡,§] Eckhard Vogel,[*,‡] and Egon Hassel[§]

[†]Vattenfall Europe PowerConsult GmbH, Kraftwerkstr. 22, D-03226 Vetschau, Germany

[‡]Institute of Chemistry, University of Rostock, A.-Einstein-Str. 3a, D-18059 Rostock, Germany

[§]Technical Thermodynamics, University of Rostock, A.-Einstein-Str. 2, D-18059 Rostock, Germany

ABSTRACT: An apparatus combining a vibrating-wire viscometer and a single-sinker densimeter was used to provide accurate $\eta\rho pT$ data for four isotherms on ethane at (293.15, 307.15 [ethane 3.5 and 5.0], and 423.15) K and five isotherms on propane at (273.15, 298.15, 366.15, 373.15, and 423.15) K. The maximum pressure was chosen to be about 95 % of the saturated vapor pressure for the subcritical isotherms and 30 MPa at maximum for the supercritical isotherms. The relative uncertainty in the density is estimated to be less than ± 0.1 %, except for the low-density range. Near the critical region, allocation errors for temperature and pressure have a significant impact on the uncertainty of the experimental densities. The density data agree within ± 0.1 %, when comparing them with values calculated from the equations of state by Bücker and Wagner (2006) for ethane and by Lemmon et al. (2009) for propane, excluding the low-density and the near-critical regions. The near-critical isotherms at 307.15 K for ethane and at 373.15 K for propane reveal differences of +2.1 % and +1.2 %, respectively, in accordance with the estimated maximum total uncertainties of the experimental $p\rho T$ data for these isotherms. The viscosity measurements are characterized by a relative uncertainty of ± (0.25 to 0.3) %, only increased by 0.04 % in the near-critical region due to the allocation errors arising from the temperature and density measurements. The new viscosity data and additionally re-evaluated earlier data of our group are compared with the viscosity surface correlations by Hendl et al. (1994) for ethane and by Scalabrin et al. (2006) for propane as well as with selected experimental data for the low-density region. For ethane, the maximum deviations of the new data exceed the stated uncertainty of ± 2.5 % for the viscosity surface correlation. For propane, the deviations do not exceed ± 0.7 %, except for the near-critical isotherm at 373.15 K. The effect of the critical enhancement became evident for the near-critical isotherms, about 2 % for ethane at 307.15 K and about 1 % for propane at 373.15 K. The new viscosity data should be used to improve the viscosity surface correlations available in the literature.

INTRODUCTION

Ethane and propane are very important working fluids in various industries, for example, in the petrochemistry or the natural gas industry. Reliable thermophysical properties are essential for designing, operating, maintaining, or retrofitting purposes of technical equipment dealing with these fluids. In addition, such properties are strongly needed both in process simulations and in computational fluid dynamics as well as for comparisons with theoretically calculated values of them. Accurately measured data determined by means of high-precision experimental equipment are the basis for state-of-the-art equations of state[1,2] and viscosity surface correlations.[3,4]

Recently, Seibt et al.[5] designed a measuring apparatus for the precise simultaneous determination of viscosity and density. The implemented viscometer makes use of the vibrating-wire technique and is based on the experiences gained with this method in measurements on gaseous fluids by Wilhelm et al.[6,7] In principle, both viscosity and density could be deduced from the parameters of the recorded oscillation curves of the vibrating wire. In doing so, the density can only be obtained with a comparably large uncertainty. But the working equation for the evaluation of the measurements with the vibrating-wire viscometer requires the fluid density to be known with an uncertainty as low as possible. Hence, the density is mostly inferred using measured values for pressure and temperature in combination with an accurate equation of state. Nevertheless, because of the uncertainties of the measured temperatures and pressures, the uncertainty of the finally derived viscosity values is increased, if the density is determined in this manner. Therefore, the viscometer was supplemented by an accurate single-sinker densimeter to reduce the influence of an increased uncertainty of the density, particularly in the near-critical region. A detailed description of the experimental equipment was reported by Seibt et al.[5] and primarily in the thesis by Seibt[8] so that here only basic essentials are depicted.

Apart from the low-density region, the relative uncertainty of the density measurements with the single-sinker method is expected to amount to ± 0.1 %, so that the relative uncertainty in the viscosity could achieve ± 0.3 %. Performance tests with measurements on helium and nitrogen were reported by Seibt et al.[5]

Special Issue: John M. Prausnitz Festschrift

Received: November 1, 2010
Accepted: January 18, 2011
Published: March 23, 2011

In this paper, new density and viscosity measurements on ethane and propane are evaluated to extend the database for these thermophysical properties. Furthermore, older measurements by Wilhelm et al.[9] on ethane and by Wilhelm and Vogel[10] on propane, using the older vibrating-wire viscometer as well as temperature and pressure measurements for the determination of the required density, were re-evaluated. The results have been reported in separate corrections.[11,12] The re-evaluation concerns the determination of the wire radius by an improved calibration (see below) as well as the calculation of the density by means of the most recent equation of state in the case of propane.[2] The new and re-evaluated data are used to test, particularly in the vicinity of the critical point, the performance of the equations of state and of the viscosity surface correlations.

■ EXPERIMENTAL SECTION

Vibrating-Wire Viscometer. Seibt et al.[5,8] have described the details of the vibrating-wire viscometer. Hence, only the essential items of the design are necessary to be summarized. Chromel has been selected as wire material due to its comparably smooth surface. The wire with a length of 90 mm and a nominal diameter of 25 μm is symmetrically arranged in a magnetic field so that all even and the third harmonic oscillation modes are suppressed. The first oscillation mode is initiated by a sinusoidal voltage pulse with a frequency close to the resonant frequency of the wire. The oscillation following the pulse is detected by amplifying the induced voltage and measuring it as a function of time. The signal-to-noise ratio is improved by recording a hundred oscillations and averaging the measured curves within a run. Then the oscillation parameters, the logarithmic decrement Δ, and the frequency ω are determined using a nonlinear regression algorithm. The necessary working equations for calculating the viscosity η were given by Seibt et al.[5] The wire radius was obtained by means of a calibration using a value for the zero-density viscosity coefficient of helium derived by Bich et al.[13] from an ab initio potential on the basis of the kinetic theory of dilute gases ($\eta_{0,\mathrm{He},293.15\mathrm{K}}$ = 19.600 μPa·s with an uncertainty of ± 0.02 %).

For the new device, the cobalt−samarium magnets were encapsulated in magnetic stainless steel to prevent them from corrosion and to avoid the porous magnets absorbing gas molecules. The new equipment possesses three circumferentially arranged sites for three vibrating-wire viscometers with two versions for different clamping of the lower end of the wire. Whereas in the former version of the vibrating-wire viscometer the lower end of the wire was clamped between the halves of stainless-steel stubbed cones and stressed by a weight with a mass of about 1.1 g, in the new version the lower end of the wire is clamped between glass-ceramic blocks placed at the end of a rotatable lever support implemented by means of two ruby bearings. The improved version suppresses a superimposed precession movement due to the freely suspended weight in the former version, especially in vacuo, and ensures that the direction of the oscillation is perpendicular to the magnetic field, so that the uncertainty of the vibrating-wire viscometer is reduced. All measurements of this paper on ethane and propane were performed with the new lever support.

Single-Sinker Densimeter. The measurements of the density ρ are performed by means of an accurate single-sinker measuring device covering a range of (1 to 2000) kg·m^{-3}. The single-sinker densimeter is based on the buoyancy principle and was developed at the Ruhr-University Bochum and improved by Klimeck et al.[14] (see also references therein). Its most important part is an electronically controlled magnetic suspension coupling[15] for the contactless transmission of the forces on the sinker within the pressure-tight measuring cell to a calibrated microbalance placed under ambient conditions. The challenge for designing the new combined viscometer-densimeter was to ensure that the magnetic fields of the suspension coupling and of the vibrating-wire viscometer do not mutually influence. For that purpose, a comparably long distance between the permanent magnet of the suspension coupling and the sinker in the neighborhood of the vibrating wires was chosen.

For the measuring series, a sinker made of quartz glass was used. Whereas in the case of helium[5] the density determination is distinctly influenced by absorption processes on quartz glass, the measurements on ethane and propane in this paper do not suffer from similar problems.

Temperature and Pressure Measurements. The temperature T was determined with a 100 Ω and later with a 25 Ω platinum resistance thermometer in connection with a precise resistance measuring bridge. The uncertainties of the thermometers amount to ± 26 mK for the 100 Ω thermometer in the temperature range (235 to 429) K and ± 18 mK for the 25 Ω thermometer between (235 and 505) K. Considering the uncertainty of the measuring bridge and the control accuracy of the thermostat (each ± 2 mK), the total uncertainty in the temperature measurement with the two thermometers adds up to ± 30 mK and ± 22 mK, respectively.

The temperature of the measuring cell is controlled by a custom-built oil-filled double-wall thermostat with a vacuum vessel for its insulation. The outer stage of this two-stage thermostat is operated by means of an oil thermostat with a performance of up to ± (10 to 50) mK. A heating tape regulated by a precise temperature controller within ± 10 mK acts as the inner stage of the thermostat.

The pressure p is measured with four absolute pressure transmitters, equipped with ranges of (41.4, 13.8, 2.76, and 0.689) MPa and characterized by an uncertainty of ± 0.01 % of full scale and of ± (0.03 to 0.05) % from reading. The transmitters are protected from the condensed fluid by operating them in a nitrogen-filled gas system, separated from the measuring fluid-filled system by using a high-precision differential pressure transducer. This transducer is suitable to detect pressure differences of ± 5 kPa and has been calibrated with an uncertainty of ± 0.04 % from reading, which contributes ≤ ± 0.002 % to the uncertainty in the pressure measurement for p > 0.15 MPa.

For the measurements on ethane and propane at supercritical isotherms and at pressures lower than the critical one but higher than the saturation pressure, a condensation of the measuring fluid occurs in the connecting tubes to the measuring cell. The same appears at subcritical isotherms and pressures higher than the saturation pressure in the tubes, since they are at ambient temperature, whereas the measuring cell is situated within the thermostat at a higher temperature. To take this condensation into account, a liquid-level indicator, the temperature of which is adjusted to a certain saturation temperature corresponding simultaneously to the pressure in the measuring cell, is placed in a definite position of the connecting tubes.[8] The uncertainty of the hydrostatic pressure corrections is estimated to be within ± 0.001 % of the pressure. In summary, the uncertainty for the pressure measurement amounts to ≤ ± 0.05 % of the determined pressure value.

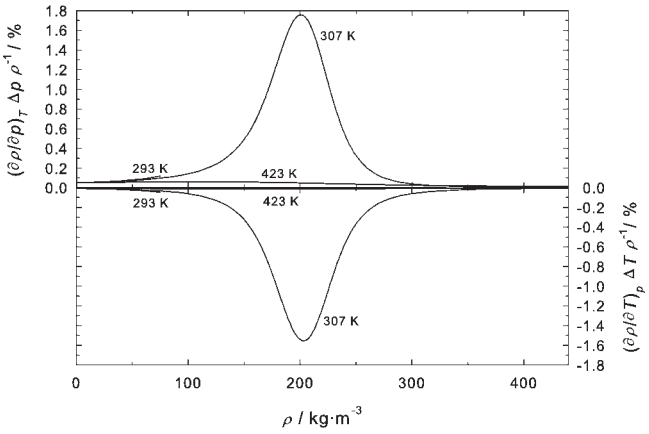

Figure 1. Allocation errors in temperature and pressure for isotherms of $p\rho T$ measurements on ethane using the equation of state by Bücker and Wagner.[1]

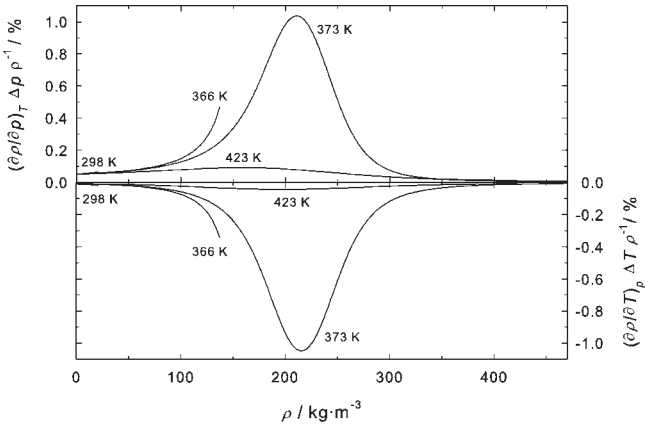

Figure 2. Allocation errors in temperature and pressure for isotherms of $p\rho T$ measurements on propane using the equation of state by Lemmon et al.[2]

Error Analysis. A sound error analysis for the newly designed viscometer−densimeter was performed by Seibt et al.[5] to demonstrate its performance for measurements on helium and nitrogen. But the situation becomes more complicated if fluids like ethane and propane are investigated, particularly in the near-critical region.

Density. The total uncertainty of the $p\rho T$ data consists of the uncertainty of the density $(\Delta\rho/\rho)$ as well as of allocation errors which are related to the uncertainties of the temperature and pressure measurements ΔT and Δp:

$$\left(\frac{\Delta\rho}{\rho}\right)_{\text{tot}} \leq \pm\sqrt{\left(\frac{\Delta\rho}{\rho}\right)^2 + \left(\frac{\partial\rho}{\partial T}\right)_p^2\frac{\Delta T^2}{\rho^2} + \left(\frac{\partial\rho}{\partial p}\right)_T^2\frac{\Delta p^2}{\rho^2}} \quad (1)$$

Here $(\Delta\rho/\rho)$ is given for the single-sinker apparatus as:

$$\frac{\Delta\rho}{\rho} \leq \pm\left|0.0526\ \% + \frac{0.07\ \%}{\rho/(10\ \text{kg}\cdot\text{m}^{-3})}\right| \quad (2)$$

The thermal expansion coefficient $(\partial\rho/\partial T)_p$ and the isothermal compressibility coefficient $(\partial\rho/\partial p)_T$, which are needed for the calculation of the allocation errors of T and p, can approximately be taken from an equation of state. Seibt et al.[5] have estimated for helium and nitrogen that in wide thermodynamic regions the total uncertainty of the density determination is $< \pm 0.1$ % for $\rho > 15\ \text{kg}\cdot\text{m}^{-3}$ due to small uncertainties of ΔT and Δp. But near the critical region, comparably high values for the partial derivatives $(\partial\rho/\partial T)_p$ and $(\partial\rho/\partial p)_T$ can occur and hence a significant impact on the uncertainty of the density results.

For ethane, the allocation errors were calculated for experimental values of temperature and pressure, considering the stated experimental uncertainties of pressure and temperature as well as $(\partial\rho/\partial T)_p$ and $(\partial\rho/\partial p)_T$ derived from the equation of state by Bücker and Wagner.[1] For the near-critical isotherm at 307 K, Figure 1 reveals a maximum of −1.56 % for the allocation error in the temperature and of +1.75 % for the allocation error in the pressure. Hence the maximum total uncertainty of experimental $p\rho T$ data (eq 1) increases up to ± 2.35 % for this isotherm.

In the case of propane, the allocation errors calculated by means of the equation of state by Lemmon et al.[2] are illustrated in Figure 2 which makes evident that the allocation errors amount up to ± 1.05 % in the near-critical region for the 373 K isotherm. This results in a maximum total uncertainty of the measured $p\rho T$ data of up to ± 1.49 %.

Table 1. Impurities in the Sample of Propane Given by the Product Specification and by the Gas Chromatographic Analysis of Linde AG, Berlin, Germany

	Linde spec	Linde GC
substance	mole fraction x	
C_3H_8	> 0.9992	> 0.99966
impurities	$10^6\ x$	
C_2H_6	≤ 200	≤ 83
C_3H_6	≤ 200	≤ 50
i-C_4H_{10}	≤ 200	≤ 47
n-C_4H_{10}	≤ 50	≤ 60
$C_4 + C_5$ (unsat.)	≤ 50	≤ 20
i-C_5H_{12}		≤ 10
n-C_5H_{12}		≤ 10
n-C_6H_{14}		≤ 10
H_2	≤ 10	≤ 1
O_2		≤ 1
N_2	≤ 50	≤ 1
CO_2	≤ 20	≤ 1
CO		≤ 1
S	≤ 1	
H_2O	≤ 10	≤ 45

With regard to the large impact of the experimental uncertainties in temperature and pressure on the total uncertainty of the $p\rho T$ data for the near-critical isotherms, the influence of impurities was investigated exemplarily for propane. The impurities given for the product specification as well as for the gas chromatographic analysis of the used propane sample are listed in Table 1. The purity is a little better according to the GC analysis (uncertainty of ± 2 % for impurities with a mole fraction $x > 5\cdot10^{-6}$) compared with the declared product specification. In addition, a sample with artificial impurities of $x = 100\cdot10^{-6}$

dx.doi.org/10.1021/je101178u |J. Chem. Eng. Data 2011, 56, 1476–1493

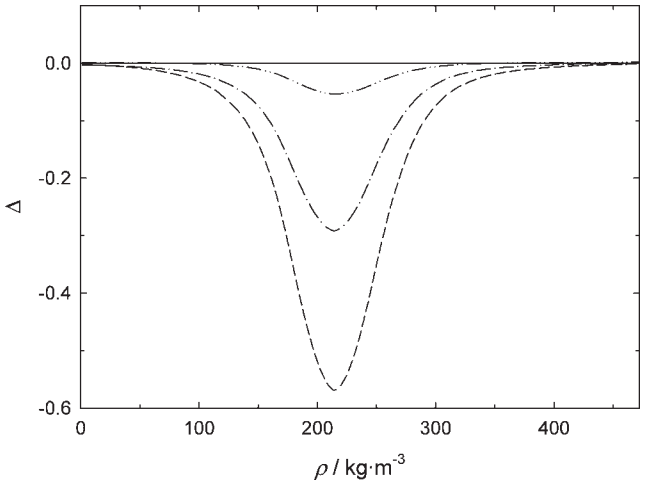

Figure 3. Comparison of calculated values for the density of contaminated samples of propane (equation of state by Kunz et al.[16]) with calculated densities for pure propane (equation of state by Lemmon et al.[2]) at 373.15 K. Deviations: $\Delta = 100(\rho_{cal,cont} - \rho_{cal,pure})/\rho_{cal,pure}$. —···—, gas chromatographic analysis by Linde; —·—, artificial composition; — — —, product specification by Linde.

for ethane and $x = 50 \cdot 10^{-6}$ for iso-butane, *n*-butane, and water was considered. Then the densities of the contaminated propane samples were calculated by means of the equation of state by Kunz et al.[16] and compared with the density obtained from the equation of state for pure propane by Lemmon et al.[2] The comparison given for the 373 K isotherm of propane is shown in Figure 3 for the artificial composition as well as for the product specification and for the gas chromatographic analysis of the supplier Linde AG, Berlin, Germany. Maximum differences occur for the composition according to the product specification, whereas the composition corresponding to the GC analysis reveals differences < −0.06 %. On the basis that the composition of the used sample corresponds to the results of the GC analysis, the densities obtained from the measurements were not corrected because of the small amount of impurities. Nevertheless, there is a certain impact of impurities in the near-critical region.

Viscosity. The total uncertainty in the viscosity consists of the uncertainty in the viscosity measurement itself as well as of the allocation errors which are related to the uncertainties of the temperature and density measurements ΔT and $\Delta\rho$ considering the temperature and density dependence of the viscosity:

$$\left(\frac{\Delta\eta}{\eta}\right)_{tot} = \left|\sqrt{\left(\frac{\Delta\eta}{\eta}\right)^2 + \left(\frac{\partial\eta}{\partial T}\right)_\rho^2 \frac{\Delta T^2}{\eta^2} + \left(\frac{\partial\eta}{\partial\rho}\right)_T^2 \frac{\Delta\rho^2}{\eta^2}}\right| \quad (3)$$

It is very disadvantageous if the density, which is needed for the evaluation of the viscosity determination, is derived from temperature and pressure measurements using an equation of state, particularly in the near-critical region due to the increase of the allocation errors in temperature and pressure (see above). But a simultaneous measurement of density and viscosity improves distinctly the situation, for which Seibt et al.[5] provided an estimation of the relative uncertainty in the viscosity measurement $(\Delta\eta/\eta)$ using an analysis of multivariate functions. As a result, the viscosity measurement is characterized by a relative uncertainty of $(\Delta\eta/\eta) \leq \pm$ (0.25 to 0.3) %, if an uncertainty of ≤ 0.1 % can be assumed for the density measurement.

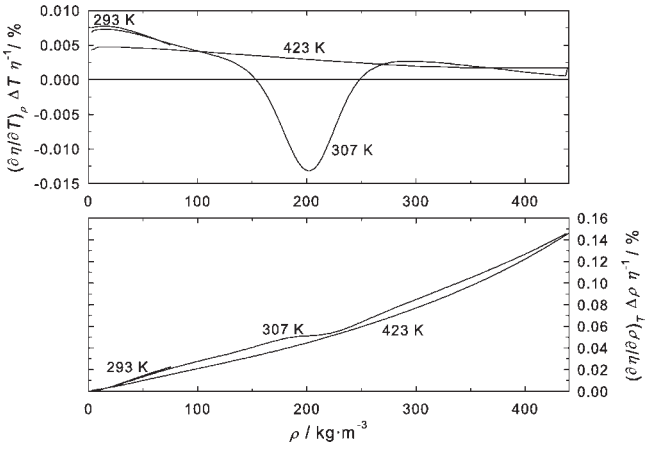

Figure 4. Allocation errors in temperature and density for isotherms of $\eta\rho T$ measurements on ethane using the viscosity surface correlation by Hendl et al.[3]

The allocation errors were calculated for experimental values of temperature and density, considering the stated experimental uncertainties of temperature and density as well as the partial derivatives $(\partial\eta/\partial T)_\rho$ and $(\partial\eta/\partial\rho)_T$ derived from the available viscosity surface correlations of ethane[3] and propane.[4] Their impact on the total uncertainty of the viscosity is virtually insignificant due to the comparably small values of $(\partial\eta/\partial T)_\rho$ and $(\partial\eta/\partial\rho)_T$, even in the near-critical region. The reason is that the critical enhancement of viscosity is small in the considered region. Its contribution amounts to about 1 % for the critical density if the temperature is 1 % higher than the critical temperature. In addition, the viscosity surface correlation of propane by Scalabrin et al.[4] does not include a contribution for the critical enhancement at all, whereas the correlation for ethane by Hendl et al.[3] takes into account the critical enhancement. Hence the allocation errors are illustrated only for ethane in Figure 4. The figure reveals for the near-critical isotherm 307.15 K a maximum of −0.013 % for the allocation error in the temperature, whereas that in the density increases approximately from +0.05 % for the critical density to +0.15 % at the highest densities. Thus the analysis leads to a maximum total uncertainty $(\Delta\eta/\eta)_{tot} \leq \pm$ (0.29 to 0.34) % for the experimental $\eta\rho T$ data (eq 3) to be compared with $(\Delta\eta/\eta) \leq \pm$ (0.25 to 0.3) % for the uncertainty in the viscosity measurement itself.

■ MEASUREMENTS AND RESULTS

The procedure of the isothermal series of measurements has already been described by Seibt et al.[5] A series is always started with the determination of the logarithmic decrement Δ_0 and of the sinker mass $m_{s,vac}$ in vacuo. Then at the beginning of the series, the measuring apparatus is filled with the fluid up to the highest pressure, and the first experimental point is carried out. The further individual points of the isothermal series are performed after reducing the pressure by a discharge of the fluid according to the measuring program. For each experimental point, the thermodynamic equilibrium has to be attained which needs about several hours at the highest densities and in the near-critical region but reduces to about half an hour at low densities. An experimental point comprises the determination of the logarithmic decrement Δ and of the frequency ω, using runs of a hundred oscillations at different initial amplitudes, as well as three or more weighings of the sinker mass $m_{s,fluid}$ in the fluid.

Concurrently, temperature T and pressure p are measured. A series of measurements is completed with a repeated measurement of the logarithmic decrement and of the sinker mass in vacuo.

The experimental viscosity η at T and p was evaluated by means of the density ρ_{exp} directly measured with the single-sinker densimeter, whereas these densities are those for the isotherm. The individual points were not exactly measured at the nominal temperature of an isotherm T_{nom} but could be kept within small deviations. The experimental viscosity data were adjusted to $\eta_{T_{nom}}$ values at the nominal temperature using a Taylor series expansion restricted to the first power in temperature. For that purpose, the following experimentally determined values of the temperature dependence for the low-density region $(\partial\eta/\partial T)_\rho$ were used: (0.027 to 0.030) μPa·s·K^{-1} by Hendl and Vogel[17] for ethane and (0.025 to 0.027) μPa·s·K^{-1} by Vogel[18] for propane. As a consequence, the pressures $p_{T_{nom}\rho_{exp}}$ at the nominal temperature change and were recalculated from the experimental densities using the equation of state by Bücker and Wagner[1] for ethane and that by Lemmon et al.[2] for propane. Furthermore, density values $\rho_{eos(T,p)}$ were calculated from the measured values for temperature T and pressure p using again the corresponding equations of state. All of these data and values are recorded below for the isothermal series of measurements on ethane and propane. It is notable that some experimental points at the lowest densities could be influenced by the slip effect; they are marked.

The measuring program on ethane and propane was partly chosen to verify the earlier results of our group reported by Wilhelm et al.[9] on ethane as well as by Wilhelm and Vogel[10] on propane. In particular, the new measurements should preferably provide improved data in the near-critical region by using the integrated density measurement. The older data by Wilhelm et al.[9,10] were obtained by means of a vibrating-wire viscometer with freely suspended weight and by using density values which were inferred from the measured values for pressure and temperature in combination with an available equation of state. For the comparison with the new viscosity values, the older data were re-evaluated. For that purpose, a recalibration of the old vibrating-wire viscometer was performed in that way that the radius of the wire was newly determined using the old measurements on argon[7] and the today accepted value for the zero-density viscosity coefficient of argon derived by Vogel et al.[19] from an ab initio potential for argon on the basis of the kinetic theory of dilute gases ($\eta_{0,Ar,298.15K}$ = 22.552 μPa·s with an uncertainty of ± 0.1 %). Furthermore, the calculation of the gas density from the measured values of temperature and of pressure was changed for propane so that the new equation of state by Lemmon et al.[2] was used instead of that by Span and Wagner.[20] For ethane the equation of state by Bücker and Wagner[1] has already been applied by Wilhelm et al.[9] As already mentioned, the improved experimental $\eta\rho pT$ data for the earlier measurements of Wilhelm et al.[9] on ethane (eight isotherms at 290 K, 300 K, 310 K, 320 K, 340 K, 370 K, 400 K, and 430 K) and of Wilhelm and Vogel[10] on propane (seven isotherms at 298.15 K, 323.15 K, 348.15 K, 366.15 K, 373.15 K, 398.15 K, and 423.15 K) are summarized in separate correction reports for ethane[11] and for propane.[12]

Ethane. Two different samples were used for the new measurements on ethane. The first sample (ethane 3.5) was supplied and certified by Linde AG, Berlin, Germany, with a mole fraction $x_{C_2H_6} > 0.9995$. According to the product specification the impurities are: $x_{C_nH_m} \leq 400\cdot10^{-6}$, $x_{H_2O} \leq 10\cdot10^{-6}$, $x_{O_2} \leq 10\cdot10^{-6}$, $x_{N_2} \leq 50\cdot10^{-6}$, and $x_{CO+CO_2} \leq 10\cdot10^{-6}$. The second

Table 2. Experimental $\eta\rho pT$ Data for Ethane 3.5 at 293.15 K

T	p	$p_{293.15K,\rho_{exp}}$	ρ_{exp}	$\rho_{eos(T,p)}$	η	$\eta_{293.15K}$
K	MPa	MPa	kg·m^{-3}	kg·m^{-3}	μPa·s	μPa·s
293.147	0.064631	0.064366	0.79811	0.80142	9.075	9.075
293.148	0.064634	0.064366	0.79811	0.80146	9.074	9.074
293.150	0.080521	0.080367	0.99778	0.99971	9.076	9.076
293.150	0.080527	0.080425	0.99851	0.99978	9.075	9.075
293.151	0.080528	0.080483	0.99923	0.9998	9.073	9.073
293.154	0.16014	0.16010	2.0005	2.0010	9.082	9.082
293.154	0.16015	0.16016	2.0012	2.0010	9.082	9.082
293.152	0.16015	0.16010	2.0005	2.0012	9.083	9.083
293.149	0.31602	0.31597	3.9991	3.9998	9.102	9.102
293.151	0.31603	0.31605	4.0002	3.9999	9.099	9.099
293.153	0.31605	0.31605	4.0002	4.0001	9.098	9.098
293.147	0.46811	0.46791	5.9992	6.0019	9.118	9.118
293.147	0.46815	0.46801	6.0006	6.0024	9.118	9.118
293.147	0.46818	0.46796	5.9999	6.0029	9.119	9.119
293.153	0.61593	0.61593	8.0004	8.0003	9.139	9.139
293.154	0.61595	0.61603	8.0018	8.0005	9.137	9.137
293.155	0.61597	0.61593	8.0004	8.0007	9.137	9.137
293.145	0.75967	0.75969	9.9972	9.9972	9.162	9.162
293.146	0.75969	0.75969	9.9972	9.9975	9.165	9.165
293.146	0.75971	0.75969	9.9972	9.9977	9.161	9.162
293.147	0.88984	0.88987	11.854	11.854	9.182	9.183
293.147	0.88987	0.88973	11.852	11.854	9.183	9.183
293.147	0.88989	0.88973	11.852	11.855	9.183	9.184
293.151	1.0363	1.0363	14.002	14.002	9.213	9.213
293.152	1.0363	1.0362	14.001	14.002	9.212	9.212
293.153	1.0364	1.0362	14.001	14.003	9.213	9.213
293.151	1.1673	1.1672	15.979	15.981	9.246	9.246
293.151	1.1674	1.1673	15.980	15.982	9.243	9.243
293.152	1.1674	1.1673	15.981	15.983	9.243	9.243
293.155	1.2938	1.2936	17.943	17.947	9.274	9.274
293.155	1.2939	1.2938	17.946	17.948	9.275	9.275
293.154	1.2940	1.2938	17.946	17.950	9.275	9.275
293.156	1.4210	1.4208	19.979	19.982	9.306	9.305
293.156	1.4210	1.4208	19.979	19.982	9.308	9.308
293.156	1.4211	1.4210	19.983	19.983	9.310	9.310
293.147	1.9925	1.9924	30.002	30.004	9.506	9.506
293.149	1.9926	1.9925	30.004	30.006	9.506	9.506
293.151	1.9927	1.9926	30.006	30.008	9.505	9.505
293.146	2.4772	2.4772	40.017	40.019	9.749	9.749
293.149	2.4774	2.4774	40.022	40.023	9.748	9.748
293.150	2.4776	2.4776	40.026	40.027	9.748	9.748
293.154	2.8796	2.8797	49.983	49.979	10.036	10.035
293.154	2.8797	2.8799	49.988	49.982	10.033	10.033
293.161	3.2118	3.2122	60.073	60.049	10.364	10.364
293.164	3.2118	3.2121	60.071	60.051	10.363	10.363
293.158	3.2118	3.2123	60.079	60.055	10.363	10.363
293.154	3.4714	3.4719	70.014	69.990	10.726	10.726
293.154	3.4716	3.4720	70.020	69.998	10.730	10.730
293.154	3.4717	3.4722	70.027	70.004	10.731	10.730
293.154	3.5771	3.5778	74.957	74.915	10.924	10.924
293.154	3.5771	3.5776	74.947	74.919	10.928	10.928

Table 3. Experimental $\eta\rho pT$ Data for Ethane 3.5 at 307.15 K

T	p	$p_{307.15K,\rho_{exp}}$	ρ_{exp}	$\rho_{eos(T,p)}$	η	$\eta_{307.15K}$
K	MPa	MPa	kg·m^{-3}	kg·m^{-3}	μPa·s	μPa·s
307.134	0.092688	0.092554	1.0967	1.0984	9.491	9.492
307.134	0.092688	0.092621	1.0975	1.0984	9.489	9.489
307.133	0.16030	0.16018	1.9070	1.9085	9.507	9.508
307.135	0.16031	0.16018	1.9070	1.9086	9.510	9.510
307.135	0.33250	0.33245	4.0065	4.0073	9.542	9.543
307.137	0.33253	0.33245	4.0065	4.0076	9.541	9.542
307.134	0.49405	0.49391	6.0228	6.0248	9.573	9.573
307.136	0.49406	0.49397	6.0235	6.0249	9.572	9.572
307.148	0.65003	0.65001	8.0195	8.0198	9.604	9.604
307.147	0.65003	0.64995	8.0188	8.0199	9.604	9.604
307.148	0.80048	0.80041	9.9903	9.9913	9.636	9.636
307.149	0.80049	0.80035	9.9895	9.9914	9.635	9.635
307.148	0.80049	0.80041	9.9903	9.9914	9.639	9.639
307.144	0.95925	0.95920	12.124	12.125	9.674	9.674
307.144	0.95926	0.95920	12.124	12.125	9.674	9.674
307.143	0.95928	0.95913	12.123	12.125	9.675	9.675
307.136	1.0945	1.0944	13.987	13.989	9.708	9.709
307.137	1.0945	1.0945	13.988	13.989	9.709	9.710
307.141	1.2338	1.2338	15.953	15.955	9.745	9.746
307.142	1.2339	1.2339	15.955	15.955	9.746	9.746
307.142	1.3434	1.3434	17.536	17.537	9.778	9.778
307.142	1.3434	1.3434	17.536	17.537	9.778	9.778
307.144	1.5026	1.5024	19.889	19.894	9.828	9.828
307.145	1.5026	1.5024	19.889	19.893	9.829	9.830
307.130	2.1342	2.1345	30.051	30.050	10.064	10.065
307.133	2.1342	2.1344	30.049	30.049	10.065	10.066
307.121	2.6736	2.6742	40.038	40.035	10.340	10.341
307.123	2.6737	2.6742	40.039	40.037	10.343	10.344
307.135	2.6741	2.6743	40.040	40.041	10.340	10.340
307.133	2.6741	2.6743	40.040	40.041	10.343	10.344
307.145	3.1384	3.1382	50.008	50.016	10.663	10.663
307.145	3.1384	3.1381	50.006	50.014	10.662	10.662
307.144	3.1385	3.1384	50.012	50.018	10.660	10.660
307.141	3.5394	3.5396	60.147	60.149	11.027	11.027
307.143	3.5397	3.5398	60.154	60.155	11.031	11.031
307.137	3.8875	3.8890	70.711	70.673	11.452	11.452
307.137	3.8908	3.8924	70.823	70.782	11.456	11.456
307.157	4.1495	4.1505	80.267	80.218	11.884	11.883
307.145	4.1504	4.1516	80.309	80.269	11.891	11.891
307.143	4.1510	4.1520	80.328	80.294	11.889	11.889
307.142	4.1513	4.1524	80.342	80.311	11.886	11.887
307.163	4.3286	4.3286	88.031	88.008	12.259	12.258
307.157	4.3295	4.3295	88.072	88.059	12.260	12.260
307.155	4.3300	4.3301	88.099	88.086	12.266	12.266
307.152	4.3303	4.3304	88.116	88.107	12.265	12.265
307.150	4.3313	4.3315	88.167	88.159	12.265	12.265
307.145	4.5136	4.5146	97.860	97.810	12.775	12.775
307.145	4.5154	4.5162	97.954	97.917	12.783	12.783
307.145	4.5166	4.5174	98.024	97.991	12.786	12.786
307.145	4.5175	4.5183	98.079	98.046	12.789	12.789
307.146	4.5184	4.5192	98.129	98.095	12.791	12.791
307.159	4.7359	4.7363	113.820	113.738	13.711	13.711

Table 3. Continued

T	p	$p_{307.15K,\rho_{exp}}$	ρ_{exp}	$\rho_{eos(T,p)}$	η	$\eta_{307.15K}$
K	MPa	MPa	kg·m^{-3}	kg·m^{-3}	μPa·s	μPa·s
307.157	4.7362	4.7367	113.852	113.775	13.711	13.711
307.155	4.9385	4.9392	140.104	139.887	15.520	15.520
307.153	4.9386	4.9393	140.112	139.931	15.516	15.516
307.152	4.9386	4.9393	140.112	139.939	15.516	15.516
307.139	5.0167	5.0195	165.654	164.677	17.665	17.665
307.139	5.0170	5.0194	165.625	164.814	17.660	17.660
307.141	5.0172	5.0194	165.641	164.826	17.663	17.664
307.160	5.0423	5.0430	183.065	181.475	19.327	19.326
307.162	5.0424	5.0430	183.021	181.371	19.323	19.323
307.164	5.0424	5.0429	182.964	181.182	19.321	19.321
307.146	5.0483	5.0511	192.228	189.299	20.280	20.280
307.148	5.0487	5.0511	192.185	189.550	20.275	20.275
307.148	5.0488	5.0510	192.154	189.652	20.258	20.258
307.149	5.0489	5.0510	192.131	189.632	20.258	20.258
307.147	5.0568	5.0588	202.654	200.232	21.368	21.368
307.148	5.0570	5.0588	202.599	200.371	21.358	21.358
307.142	5.0571	5.0603	204.743	201.370	21.584	21.585
307.145	5.0571	5.0603	204.709	200.910	21.575	21.576
307.141	5.0572	5.0604	204.805	201.652	21.592	21.592
307.149	5.0574	5.0588	202.583	200.795	21.326	21.326
307.150	5.0574	5.0587	202.521	200.638	21.325	21.325
307.152	5.0575	5.0587	202.456	200.475	21.325	21.324
307.142	5.0619	5.0642	210.139	208.170	22.189	22.190
307.140	5.0620	5.0642	210.110	208.532	22.193	22.194
307.145	5.0626	5.0641	209.963	208.670	22.147	22.148
307.148	5.0628	5.0641	209.982	208.463	22.155	22.155
307.148	5.0628	5.0641	209.961	208.446	22.147	22.147
307.178	5.1077	5.1050	242.924	242.573	25.789	25.788
307.178	5.1078	5.1052	243.012	242.648	25.798	25.797
307.178	5.1078	5.1050	242.960	242.630	25.792	25.792
307.178	5.1079	5.1051	243.000	242.654	25.790	25.790
307.169	5.1623	5.1606	259.321	259.105	27.813	27.812
307.174	5.1628	5.1609	259.389	259.083	27.816	27.815
307.174	5.1630	5.1610	259.401	259.124	27.810	27.809
307.176	5.1633	5.1610	259.396	259.113	27.796	27.795
307.172	5.3502	5.3481	282.102	281.972	31.093	31.092
307.173	5.3504	5.3483	282.116	281.976	31.094	31.093
307.174	5.3509	5.3485	282.128	281.997	31.103	31.102
307.175	5.3510	5.3486	282.136	281.994	31.098	31.098
307.176	5.6506	5.6481	299.179	299.068	33.890	33.890
307.178	5.6511	5.6483	299.189	299.076	33.886	33.885
307.180	5.6520	5.6487	299.204	299.098	33.924	33.923
307.179	5.6522	5.6488	299.208	299.112	33.908	33.907
307.056	6.3046	6.3282	319.833	319.787	37.735	37.738
307.057	6.3047	6.3285	319.840	319.784	37.717	37.720
307.057	6.3056	6.3289	319.850	319.804	37.763	37.765
307.232	6.3418	6.3262	319.788	319.715	37.734	37.731
307.262	7.6268	7.5982	341.100	341.075	42.259	42.256
307.260	7.6306	7.6022	341.152	341.131	42.300	42.297
307.262	7.6310	7.6030	341.162	341.129	42.301	42.298
307.183	9.6377	9.6274	361.481	361.478	47.260	47.259
307.232	9.6499	9.6281	361.486	361.450	47.283	47.281

dx.doi.org/10.1021/je101178u |J. Chem. Eng. Data 2011, 56, 1476–1493

Table 3. Continued

T	p	$p_{307.15K,\rho_{exp}}$	ρ_{exp}	$\rho_{eos(T,p)}$	η	$\eta_{307.15K}$
K	MPa	MPa	kg·m^{-3}	kg·m^{-3}	μPa·s	μPa·s
307.171	12.510	12.508	380.388	380.358	52.571	52.570
307.171	12.510	12.507	380.383	380.354	52.569	52.569
307.171	12.511	12.509	380.392	380.361	52.554	52.554
307.070	15.936	15.941	396.414	396.531	57.680	57.682
307.082	15.944	15.981	396.579	396.542	57.677	57.679
307.091	15.954	15.986	396.599	396.569	57.670	57.672
307.111	15.965	15.987	396.601	396.578	57.693	57.694
307.142	15.977	15.985	396.595	396.576	57.652	57.653

Table 4. Experimental $\eta\rho pT$ Data for Ethane 5.0 at 307.15 K

T	p	$p_{307.15K,\rho_{exp}}$	ρ_{exp}	$\rho_{eos(T,p)}$	η	$\eta_{307.15K}$
K	MPa	MPa	kg·m^{-3}	kg·m^{-3}	μPa·s	μPa·s
307.140	0.097868	0.097810	1.1594	1.1601	9.507[a]	9.507[a]
307.142	0.097883	0.097810	1.1594	1.1603	9.507[a]	9.508[a]
307.141	0.16682	0.16671	1.9856	1.9870	9.530	9.531
307.141	0.16683	0.16677	1.9863	1.9871	9.528	9.529
307.146	0.32758	0.32738	3.9439	3.9455	9.566	9.566
307.146	0.32759	0.32738	3.9439	3.9456	9.566	9.566
307.147	0.78872	0.78848	9.8322	9.8355	9.663	9.663
307.148	0.78874	0.78870	9.8351	9.8357	9.665	9.665
307.141	1.4695	1.4693	19.394	19.397	9.854	9.855
307.142	1.4697	1.4695	19.396	19.400	9.856	9.856
307.138	2.6534	2.6536	39.629	39.629	10.380	10.380
307.139	2.6537	2.6537	39.631	39.634	10.379	10.379
307.145	3.8158	3.8156	68.316	68.326	11.418	11.419
307.146	3.8220	3.8217	68.511	68.525	11.429	11.430
307.139	4.5564	4.5577	100.499	100.427	13.020	13.021
307.140	4.5569	4.5581	100.521	100.451	13.022	13.022
307.130	5.0052	5.0089	160.457	159.564	17.291	17.292
307.134	5.0054	5.0089	160.473	159.529	17.294	17.294
307.142	5.0470	5.0501	191.037	188.237	20.217	20.218
307.143	5.0472	5.0502	191.169	188.278	20.230	20.230
307.135	5.0557	5.0602	204.534	200.431	21.674	21.675
307.137	5.0558	5.0602	204.598	200.318	21.679	21.679
307.134	5.0572	5.0601	204.501	202.626	21.674	21.675
307.143	5.0583	5.0621	207.310	203.266	21.985	21.985
307.141	5.0584	5.0622	207.441	203.136	22.000	22.000
307.143	5.0585	5.0620	207.173	203.154	21.995	21.995
307.136	5.0609	5.0654	211.657	207.631	22.546	22.547
307.138	5.0612	5.0654	211.736	207.697	22.552	22.552
307.140	5.0614	5.0655	211.805	207.692	22.553	22.553
307.126	5.1804	5.1876	264.291	263.671	28.523	28.524
307.136	5.1812	5.1874	264.252	263.562	28.525	28.525
307.138	5.1812	5.1871	264.206	263.502	28.524	28.524
307.123	5.3606	5.3691	283.708	283.417	31.438	31.439
307.146	5.3627	5.3679	283.622	283.284	31.404	31.404
307.146	5.3632	5.3685	283.666	283.320	31.399	31.399
307.145	5.3638	5.3694	283.730	283.380	31.412	31.413
307.121	5.6630	5.6739	300.263	300.045	34.197	34.198
307.128	5.6648	5.6740	300.270	300.066	34.158	34.158

Table 4. Continued

T	p	$p_{307.15K,\rho_{exp}}$	ρ_{exp}	$\rho_{eos(T,p)}$	η	$\eta_{307.15K}$
K	MPa	MPa	kg·m^{-3}	kg·m^{-3}	μPa·s	μPa·s
307.132	5.6656	5.6742	300.276	300.067	34.172	34.172
307.125	5.6671	5.6739	300.265	300.185	34.175	34.176
307.144	6.3369	6.3439	320.187	320.060	37.808	37.808
307.144	6.3376	6.3447	320.206	320.078	37.829	37.830
307.144	6.3389	6.3460	320.235	320.106	37.839	37.839
307.143	6.3400	6.3472	320.260	320.135	37.831	37.831
307.141	7.6910	7.7001	342.393	342.310	42.561	42.562
307.141	7.6917	7.7008	342.402	342.320	42.568	42.568
307.141	7.6926	7.7017	342.413	342.331	42.566	42.566
307.025	9.6514	9.7050	362.101	361.995	47.373	47.377
307.026	9.6562	9.7036	362.090	362.032	47.418	47.421
307.054	9.6595	9.7031	362.086	361.986	47.424	47.427
307.089	12.525	12.559	380.663	380.606	52.628	52.629
307.097	12.527	12.558	380.661	380.600	52.633	52.634
307.152	12.532	12.544	380.585	380.516	52.758	52.758
307.152	12.533	12.545	380.588	380.519	52.681	52.681
307.131	12.536	12.554	380.638	380.580	52.577	52.578
307.131	12.536	12.554	380.638	380.577	52.599	52.600
307.212	12.540	12.549	380.613	380.436	52.626	52.624
307.097	16.841	16.874	400.063	400.024	58.880	58.882
307.102	16.843	16.875	400.066	400.024	58.854	58.855
307.116	16.849	16.875	400.066	400.025	58.868	58.869
307.118	16.850	16.874	400.065	400.027	58.815	58.816
307.121	16.852	16.875	400.067	400.027	58.813	58.813
307.127	16.855	16.875	400.068	400.029	58.945	58.946
307.128	16.856	16.876	400.071	400.031	58.845	58.845
307.131	16.857	16.876	400.073	400.032	58.846	58.846
307.133	16.858	16.877	400.075	400.032	58.844	58.844
307.143	19.733	19.746	410.021	409.991	62.384	62.384
307.143	19.735	19.746	410.023	409.996	62.405	62.406
307.142	19.736	19.749	410.030	410.002	62.362	62.362
307.142	19.738	19.750	410.034	410.007	62.419	62.419
307.142	19.739	19.751	410.039	410.011	62.403	62.403
307.130	23.193	23.210	420.157	420.138	66.334	66.334
307.133	23.194	23.209	420.154	420.135	66.330	66.330
307.136	23.195	23.210	420.156	420.136	66.295	66.295
307.135	23.195	23.210	420.157	420.136	66.343	66.344
307.130	24.515	24.530	423.617	423.604	67.755	67.755
307.134	24.516	24.530	423.617	423.602	67.777	67.777
307.132	24.516	24.530	423.615	423.603	67.807	67.807
307.135	24.517	24.530	423.617	423.603	67.805	67.805
307.137	24.519	24.531	423.619	423.606	67.736	67.737
307.136	24.519	24.531	423.619	423.606	67.751	67.751
307.143	25.866	25.875	426.955	426.944	69.129	69.129
307.143	25.869	25.877	426.961	426.950	69.140	69.140
307.142	25.871	25.879	426.966	426.956	69.063	69.064
307.142	25.872	25.881	426.969	426.959	69.106	69.106
307.142	29.044	29.053	434.215	434.206	72.346	72.346
307.141	29.049	29.057	434.225	434.218	72.317	72.318
307.141	29.055	29.063	434.238	434.230	72.269	72.270
307.142	29.973	29.978	436.186	436.185	73.167	73.168
307.142	29.973	29.978	436.185	436.184	73.250	73.251

dx.doi.org/10.1021/je101178u |J. Chem. Eng. Data 2011, 56, 1476–1493

Table 4. Continued

T	p	$p_{307.15K,\rho_{exp}}$	ρ_{exp}	$\rho_{eos(T,p)}$	η	$\eta_{307.15K}$
K	MPa	MPa	kg·m^{-3}	kg·m^{-3}	μPa·s	μPa·s
307.142	29.974	29.980	436.189	436.187	73.137	73.137
307.142	29.974	29.980	436.189	436.187	73.185	73.185
307.142	29.979	29.979	436.187	436.197	73.234	73.234

[a] Influenced by slip.

Table 5. Experimental $\eta\rho pT$ Data for Ethane 5.0 at 423.15 K

T	p	$p_{423.15K,\rho_{exp}}$	ρ_{exp}	$\rho_{eos(T,p)}$	η	$\eta_{423.15K}$
K	MPa	MPa	kg·m^{-3}	kg·m^{-3}	μPa·s	μPa·s
423.146	0.095803	0.095833	0.82091	0.82066	12.763[a]	12.763[a]
423.139	0.095803	0.095748	0.82018	0.82067	12.766[a]	12.766[a]
423.152	0.11758	0.11747	1.0068	1.0077	12.774[a]	12.774[a]
423.143	0.11759	0.11773	1.0090	1.0079	12.767[a]	12.767[a]
423.138	0.11760	0.11764	1.0082	1.0079	12.768[a]	12.769[a]
423.150	0.22659	0.22659	1.9470	1.9470	12.796	12.796
423.152	0.22661	0.22676	1.9485	1.9472	12.798	12.798
423.151	0.22662	0.22676	1.9485	1.9472	12.798	12.798
423.130	0.45931	0.45937	3.9693	3.9690	12.842	12.843
423.137	0.45935	0.45946	3.9701	3.9692	12.842	12.842
423.152	0.69249	0.69162	6.0097	6.0173	12.898	12.898
423.149	0.69252	0.69195	6.0126	6.0177	12.891	12.891
423.150	0.91658	0.91603	8.0031	8.0080	12.935	12.935
423.157	0.91663	0.91595	8.0024	8.0083	12.940	12.940
423.137	1.1367	1.1367	9.9843	9.9849	12.976	12.976
423.135	1.1368	1.1365	9.9828	9.9857	12.976	12.976
423.132	1.3578	1.3576	11.990	11.992	13.025	13.025
423.140	1.3579	1.3579	11.993	11.993	13.025	13.025
423.147	1.5765	1.5765	13.999	13.998	13.064	13.064
423.142	1.5766	1.5765	13.999	13.999	13.066	13.066
423.163	1.7946	1.7944	16.020	16.021	13.118	13.117
423.157	1.7949	1.7950	16.025	16.024	13.114	13.114
423.193	2.0070	2.0071	18.014	18.011	13.168	13.167
423.189	2.0072	2.0072	18.015	18.013	13.169	13.167
423.192	2.2094	2.2091	19.928	19.928	13.219	13.218
423.201	2.2098	2.2092	19.929	19.931	13.218	13.217
423.130	3.2425	3.2430	30.033	30.030	13.519	13.520
423.140	3.2438	3.2445	30.048	30.042	13.509	13.509
423.133	4.1633	4.1645	39.495	39.485	13.815	13.816
423.134	4.1633	4.1644	39.494	39.484	13.816	13.816
423.173	4.5515	4.5515	43.602	43.598	13.955	13.954
423.174	4.5552	4.5553	43.642	43.638	13.963	13.962
423.170	5.9116	5.9106	58.665	58.672	14.544	14.544
423.166	5.9145	5.9143	58.707	58.706	14.552	14.551
423.267	6.7491	6.7462	68.424	68.424	14.973	14.970
423.284	6.7504	6.7469	68.432	68.435	14.976	14.972
423.175	7.5297	7.5280	77.889	77.901	15.419	15.418
423.180	7.5311	7.5301	77.915	77.917	15.419	15.418
423.155	8.2989	8.2985	87.517	87.519	15.900	15.900
423.149	8.3009	8.3008	87.546	87.547	15.904	15.904
423.137	9.2356	9.2359	99.586	99.590	16.556	16.557
423.126	9.2369	9.2385	99.621	99.612	16.554	16.555

Table 5. Continued

T	p	$p_{423.15K,\rho_{exp}}$	ρ_{exp}	$\rho_{eos(T,p)}$	η	$\eta_{423.15K}$
K	MPa	MPa	kg·m^{-3}	kg·m^{-3}	μPa·s	μPa·s
423.103	10.729	10.733	119.476	119.464	17.750	17.751
423.102	10.732	10.732	119.465	119.496	17.738	17.739
423.152	12.215	12.215	139.509	139.507	19.096	19.096
423.135	12.216	12.218	139.549	139.544	19.091	19.091
423.137	13.725	13.727	159.706	159.702	20.619	20.620
423.142	13.726	13.728	159.722	159.713	20.615	20.615
423.141	15.324	15.325	180.142	180.144	22.340	22.340
423.141	15.325	15.327	180.168	180.161	22.340	22.340
423.160	16.992	16.990	199.904	199.905	24.200	24.199
423.163	16.993	16.991	199.911	199.919	24.207	24.207
423.170	16.994	16.992	199.925	199.926	24.204	24.203
423.156	18.870	18.872	220.003	219.975	26.316	26.315
423.183	18.874	18.874	220.020	219.980	26.316	26.315
423.200	18.882	18.878	220.065	220.047	26.335	26.333
423.139	21.030	21.034	240.207	240.188	28.700	28.700
423.133	21.030	21.034	240.204	240.189	28.702	28.703
423.156	23.413	23.414	259.265	259.253	31.192	31.192
423.155	23.415	23.415	259.275	259.265	31.196	31.196
423.152	26.527	26.527	280.132	280.131	34.252	34.251
423.146	26.528	26.529	280.144	280.143	34.243	34.243
423.240	30.182	30.162	300.101	300.106	37.570	37.567
423.170	30.184	30.181	300.195	300.191	37.562	37.562
423.172	30.188	30.183	300.204	300.205	37.578	37.578
423.232	30.190	30.174	300.162	300.152	37.573	37.570

[a] Influenced by slip.

sample (ethane 5.0) supplied by Gerling Holz & Co., Hamburg, Germany, with a certified purity $x_{C_2H_6} > 0.999985$ was utilized for the supercritical isotherms. Its impurities consist of: $x_{C_nH_m} < 6 \cdot 10^{-6}$ (analyzed to CH_4, C_2H_4, C_2H_2, C_3H_8, C_4), $x_{H_2O} < 3 \cdot 10^{-6}$, $x_{O_2} < 1 \cdot 10^{-6}$, $x_{N_2} < 3 \cdot 10^{-6}$, and $x_{CO+CO_2} < 2 \cdot 10^{-6}$.

Four isothermal series of measurements on ethane were carried out, one at a subcritical temperature (293.15 K) and three at supercritical temperatures (two samples at 307.15 K and one at 423.15 K). The maximum pressure was chosen to be about 95 % of the saturated vapor pressure for the subcritical isotherm and up to 15 or 30 MPa for the supercritical isotherms. The two isothermal series of measurements at 307.15 K are only 1.83 K away from the critical temperature T_c = 305.322 K. The results of the measuring series on ethane are summarized in Tables 2 to 5.

Propane. A sample (propane 3.5) supplied by Linde AG, Berlin, Germany, with a certified purity of $x_{C_3H_8} > 0.9992$ was used. As already mentioned above, its impurities according to the product specification and to the gas chromatographic analysis ($x_{C_3H_8} > 0.99966$) are given in Table 1.

Three isotherms were recorded at subcritical temperatures (273.15 K, 298.15 K, and 366.15 K) and two at supercritical ones (373.15 K and 423.15 K). The subcritical isotherms cover ranges up to about 95 % of the saturated vapor pressure, whereas the supercritical isotherms were performed up to 30 MPa. It is to be mentioned that the first supercritical isotherm is only 3.26 K away from the critical temperature T_c = 369.89 K. The results of the five series of measurements on propane at the stated isotherms are summarized in Tables 6 to 10.

Table 6. Experimental $\eta\rho pT$ Data for Propane at 273.15 K

T	p	$p_{273.15K,\rho_{exp}}$	ρ_{exp}	$\rho_{eos(T,p)}$	η	$\eta_{273.15K}$
K	MPa	MPa	kg·m^{-3}	kg·m^{-3}	μPa·s	μPa·s
273.187	0.040893	0.040934	0.80164	0.80072	7.441[a]	7.440[a]
273.191	0.051025	0.051054	1.0020	1.0013	7.444[a]	7.443[a]
273.193	0.10083	0.10076	1.9990	2.0001	7.444	7.443
273.188	0.14969	0.14962	3.0011	3.0021	7.436	7.435
273.188	0.19712	0.19697	3.9945	3.9971	7.432	7.431
273.189	0.24395	0.24387	5.0016	5.0025	7.425	7.424
273.184	0.28937	0.28930	6.0007	6.0013	7.420	7.419
273.185	0.33381	0.33356	6.9977	7.0023	7.416	7.415
273.185	0.37683	0.37667	7.9933	7.9956	7.411	7.410
273.200	0.42011	0.42003	9.0207	9.0203	7.408	7.406
273.213	0.42013	0.42003	9.0207	9.0201	7.407	7.406
273.217	0.45966	0.45955	9.9815	9.9808	7.406	7.404
273.220	0.45970	0.45958	9.9822	9.9816	7.405	7.403

[a] Influenced by slip.

Table 7. Experimental $\eta\rho pT$ Data for Propane at 298.15 K

T	p	$p_{298.15K,\rho_{exp}}$	ρ_{exp}	$\rho_{eos(T,p)}$	η	$\eta_{298.15K}$
K	MPa	MPa	kg·m^{-3}	kg·m^{-3}	μPa·s	μPa·s
298.126	0.044444	0.044704	0.80087	0.79624	8.127[a]	8.128[a]
298.125	0.055587	0.055551	0.99693	0.99767	8.132	8.133
298.123	0.11047	0.11039	1.9989	2.0006	8.130	8.130
298.114	0.16419	0.16409	2.9981	3.0005	8.126	8.127
298.130	0.16467	0.16466	3.0089	3.0093	8.125	8.126
298.131	0.21710	0.21705	4.0022	4.0034	8.126	8.127
298.129	0.21711	0.21709	4.0029	4.0036	8.127	8.128
298.128	0.26879	0.26878	5.0013	5.0020	8.125	8.125
298.121	0.31810	0.31803	5.9708	5.9728	8.125	8.125
298.126	0.36945	0.36940	7.0017	7.0034	8.130	8.130
298.124	0.41848	0.41844	8.0059	8.0075	8.125	8.126
298.109	0.46476	0.46473	8.9725	8.9748	8.127	8.128
298.127	0.49887	0.49881	9.6967	9.6989	8.126	8.126
298.130	0.51363	0.51359	10.014	10.016	8.121	8.121
298.130	0.56005	0.55993	11.023	11.027	8.129	8.129
298.127	0.60086	0.60075	11.930	11.934	8.131	8.132
298.123	0.60418	0.60400	12.003	12.009	8.127	8.127
298.120	0.64644	0.64636	12.965	12.969	8.128	8.128
298.124	0.64649	0.64636	12.965	12.970	8.130	8.130
298.122	0.69092	0.69104	14.002	14.001	8.131	8.132
298.114	0.69211	0.69219	14.029	14.030	8.133	8.133
298.132	0.78339	0.78349	16.228	16.227	8.144	8.144
298.127	0.84886	0.84903	17.879	17.877	8.149	8.150
298.109	0.87488	0.87516	18.556	18.553	8.154	8.155
298.121	0.87848	0.87868	18.648	18.646	8.157	8.158

[a] Influenced by slip.

EVALUATION OF DATA

Density. *Ethane.* The results of the density measurements on ethane are compared with values calculated for the equation of state by Bücker and Wagner.[1] This equation is characterized by an uncertainty in the density of about ± (0.02 to 0.04) % from the melting line up to temperatures of 520 K and pressures of 30 MPa as well as by an uncertainty in pressure of ± 0.02 % for the extended critical region. The thermal behavior in these regions was determined primarily by measurements at the Ruhr-University Bochum with a two-sinker densimeter by Funke et al.[21,22] and a single-sinker densimeter by Claus et al.[23]

Table 8. Experimental $\eta\rho pT$ Data for Propane at 366.15 K

T	p	$p_{366.15K,\rho_{exp}}$	ρ_{exp}	$\rho_{eos(T,p)}$	η	$\eta_{366.15K}$
K	MPa	MPa	kg·m^{-3}	kg·m^{-3}	μPa·s	μPa·s
366.088	0.068751	0.068968	1.0047	1.0017	9.905[a]	9.907[a]
366.087	0.13665	0.13686	2.0051	2.0024	9.921	9.923
366.087	0.27015	0.27035	4.0067	4.0044	9.940	9.941
366.088	0.40036	0.40053	6.0046	6.0031	9.955	9.956
366.093	0.52684	0.52704	7.9924	7.9907	9.973	9.974
366.091	0.64983	0.64996	9.9702	9.9700	9.995	9.996
366.098	0.77222	0.77249	11.990	11.988	10.019	10.021
366.089	0.89757	0.89782	14.109	14.108	10.045	10.047
366.096	1.0042	1.0048	15.963	15.956	10.067	10.069
366.098	1.1192	1.1198	18.006	17.998	10.099	10.101
366.093	1.2217	1.2223	19.872	19.865	10.131	10.133
366.092	1.7381	1.7387	30.044	30.039	10.316	10.317
366.099	2.1808	2.1818	40.086	40.074	10.552	10.553
366.092	2.5578	2.5591	50.015	49.998	10.827	10.828
366.090	2.8805	2.8830	60.029	59.975	11.139	11.141
366.093	3.1518	3.1544	70.033	69.972	11.493	11.494
366.092	3.3782	3.3811	80.175	80.100	11.894	11.896
366.097	3.5567	3.5595	90.050	89.968	12.322	12.323
366.101	3.7013	3.7041	100.205	100.099	12.815	12.817
366.100	3.7020	3.7049	100.267	100.158	12.822	12.823

[a] Influenced by slip.

Figure 5 shows the deviations in density of the experimental data of this paper from the values calculated for the equation of state by Bücker and Wagner using the measured temperatures and pressures. Except for the low-density and the extended critical regions, the experimental density data agree with the equation of state within ± 0.1 %. The figure reveals maximum differences of about +2.1 % for the near-critical isotherm at 307.15 K in the range of the critical density (ρ_c = 206.18 kg·m^{-3}). As already stated, the maximum total uncertainty of experimental $p\rho T$ data could amount to ± 2.35 % for this isotherm. But in thermodynamic regions with high compressibility, the measured pressures should preferably be compared with calculated pressures using a special equation of state as well as the measured temperatures and densities. Figure 6 illustrates that, apart from the low-density region and some measuring points for the ethane 5.0 sample at 307.15 K and at densities higher than the critical one, experimental data and calculated values agree within ± 0.05 %.

Propane. The results of the density measurements on propane are compared with values calculated for the equation of state by Lemmon et al.[2] This equation is characterized by an uncertainty in density of ± 0.01 % in the liquid phase and of ± 0.03 % in the vapor phase up to temperatures of 350 K and pressures of 10 MPa. The uncertainty in density increases to ± 0.1 % in the extended critical region. In the vicinity of the critical point, the uncertainty in pressure amounts to ± 0.04 %.

Table 9. Experimental $\eta\rho pT$ Data for Propane at 373.15 K

T	p	$p_{373.15K,\rho_{exp}}$	ρ_{exp}	$\rho_{eos(T,p)}$	η	$\eta_{373.15K}$
K	MPa	MPa	kg·m^{-3}	kg·m^{-3}	μPa·s	μPa·s
373.137	0.070016	0.070003	1.0004	1.0006	10.081[a]	10.081[a]
373.123	0.13925	0.13924	2.0008	2.0011	10.096	10.097
373.125	0.27558	0.27558	4.0037	4.0040	10.119	10.120
373.126	0.40884	0.40876	6.0045	6.0061	10.143	10.144
373.128	0.53871	0.53860	7.9996	8.0018	10.173	10.173
373.133	0.66697	0.66693	10.017	10.018	10.198	10.198
373.132	0.73361	0.73366	11.085	11.085	10.214	10.214
373.146	0.91729	0.91757	14.099	14.095	10.262	10.262
373.133	1.0226	1.0233	15.881	15.871	10.287	10.287
373.135	1.1475	1.1478	18.031	18.026	10.325	10.326
373.121	1.2474	1.2480	19.801	19.793	10.356	10.356
373.126	1.7813	1.7818	29.954	29.948	10.576	10.576
373.130	1.7813	1.7819	29.957	29.947	10.575	10.576
373.127	2.2434	2.2442	39.982	39.969	10.831	10.832
373.122	2.2438	2.2445	39.990	39.980	10.834	10.835
373.141	2.6402	2.6409	49.858	49.842	11.127	11.128
373.141	2.6402	2.6408	49.856	49.842	11.126	11.126
373.150	2.9834	2.9843	59.751	59.722	11.464	11.464
373.147	2.9834	2.9844	59.753	59.723	11.462	11.462
373.159	3.2881	3.2887	70.030	70.003	11.861	11.861
373.168	3.2885	3.2890	70.041	70.012	11.859	11.859
373.101	3.5294	3.5313	79.736	79.700	12.268	12.269
373.099	3.5295	3.5316	79.746	79.706	12.268	12.269
373.114	3.7380	3.7398	89.698	89.655	12.730	12.731
373.106	3.7382	3.7402	89.720	89.676	12.729	12.730
373.107	3.9071	3.9093	99.518	99.463	13.226[b]	13.228[b]
373.116	3.9072	3.9091	99.505	99.452	13.232[b]	13.233[b]
373.140	4.1512	4.1525	118.628	118.535	14.312[b]	14.312[b]
373.141	4.1513	4.1526	118.636	118.541	14.308[b]	14.308[b]
373.156	4.3136	4.3146	139.148	138.932	15.607[b]	15.607[b]
373.158	4.3138	4.3146	139.152	138.950	15.605[b]	15.605[b]
373.121	4.3977	4.4007	157.947	157.541	16.917[b]	16.918[b]
373.134	4.3982	4.4006	157.919	157.480	16.909[b]	16.909[b]
373.112	4.4293	4.4329	169.087	168.518	17.730[b]	17.731[b]
373.130	4.4302	4.4329	169.072	168.451	17.719[b]	17.720[b]
373.144	4.4309	4.4329	169.051	168.399	17.720[b]	17.720[b]
373.121	4.4546	4.4582	181.487	180.470	18.760[b]	18.761[b]
373.132	4.4553	4.4582	181.456	180.468	18.759[b]	18.759[b]
373.130	4.4741	4.4773	194.680	193.215	20.022	20.022
373.139	4.4748	4.4774	194.740	193.278	20.030	20.030
373.108	4.4868	4.4920	207.643	205.626	21.350	21.351
373.113	4.4871	4.4919	207.584	205.564	21.347	21.348
373.105	4.4968	4.5027	218.113	215.662	22.473	22.474
373.113	4.4973	4.5027	218.095	215.550	22.467	22.468
373.122	4.5071	4.5122	227.140	224.482	23.470	23.471
373.125	4.5073	4.5122	227.171	224.445	23.466	23.467
373.123	4.5100	4.5150	229.692	227.144	23.762	23.763
373.125	4.5102	4.5151	229.821	227.180	23.774	23.775
373.110	4.5237	4.5302	241.880	239.668	25.190	25.191
373.118	4.5244	4.5301	241.836	239.680	25.177	25.178
373.101	4.5484	4.5560	256.611	255.183	27.013	27.014
373.111	4.5494	4.5561	256.634	255.217	26.999	27.000
373.111	4.5692	4.5763	264.609	263.467	28.060	28.061
373.115	4.5696	4.5762	264.588	263.470	28.046	28.046
373.099	4.5979	4.6061	273.294	272.553	29.252	29.254
373.109	4.5989	4.6061	273.287	272.544	29.260	29.261
373.127	4.6515	4.6572	283.680	283.148	30.780	30.780
373.130	4.6521	4.6575	283.727	283.194	30.781	30.782
373.135	4.8033	4.8093	301.877	301.514	33.692	33.692
373.145	4.8049	4.8095	301.894	301.543	33.668	33.668
373.138	5.0994	5.1058	320.902	320.675	37.057	37.057
373.156	5.1015	5.1056	320.889	320.648	37.051	37.051
373.180	5.6144	5.6147	339.536	339.381	40.755	40.755
373.183	5.6164	5.6164	339.584	339.424	40.768	40.767
373.153	5.6443	5.6521	340.592	340.360	40.963	40.963
373.079	5.6454	5.6659	340.974	340.746	41.051	41.053
373.096	5.6475	5.6646	340.939	340.723	41.036	41.038
373.120	6.5873	6.6028	360.840	360.680	45.546	45.547
373.122	6.5886	6.6035	360.852	360.695	45.528	45.529
373.064	8.1086	8.1404	381.200	381.076	50.759	50.761
373.074	8.1109	8.1401	381.197	381.076	50.767	50.769
373.072	10.446	10.482	401.460	401.355	56.732	56.734
373.079	10.449	10.483	401.469	401.363	56.740	56.742
373.055	13.791	13.841	421.334	421.235	63.462	63.465
373.067	13.797	13.841	421.333	421.246	63.425	63.427
373.094	18.523	18.565	441.166	441.087	71.273	71.275
373.097	18.526	18.567	441.173	441.094	71.273	71.274
373.086	24.950	25.008	460.907	460.825	80.055	80.057
373.089	24.953	25.008	460.907	460.830	80.240	80.241
373.093	24.957	25.010	460.912	460.836	80.218	80.220
373.097	24.959	25.010	460.912	460.837	80.132	80.134
373.110	28.926	28.975	470.686	470.615	85.312	85.313
373.112	28.927	28.973	470.682	470.615	85.262	85.263
373.115	28.928	28.975	470.686	470.614	85.364	85.365
373.117	28.929	28.975	470.686	470.614	85.300	85.301
373.109	29.778	29.830	472.624	472.550	86.256	86.257
373.111	29.780	29.829	472.623	472.553	86.262	86.263

[a] Influenced by slip. [b] Influenced possibly by convection.

The three most important $p\rho T$ data sets in developing this equation of state were obtained at the Ruhr-University Bochum[24,25] and at the National Institute of Standards and Technology (NIST) in Boulder, CO.[26] These measurements ranged over temperatures from (95 to 520) K and extended to pressures of 36 MPa. In addition, sufficient data points were measured in the critical region by these groups. Two-sinker densimeters were applied by Glos et al.[25] and McLinden,[26] whereas Claus et al.[24] used a single-sinker densimeter.

Figure 7 illustrates the deviations in density of the experimental data of this paper from the values calculated for the equation of state by Lemmon et al.[2] using the experimentally obtained pressures and temperatures. Apart from the near-critical isotherm and the low-density region, the agreement between experiment and equation of state is within ± 0.1 %. For the

dx.doi.org/10.1021/je101178u |J. Chem. Eng. Data 2011, 56, 1476–1493

Table 10. Experimental $\eta\rho pT$ Data for Propane at 423.15 K

T	p	$p_{423.15K,\rho_{exp}}$	ρ_{exp}	$\rho_{eos(T,p)}$	η	$\eta_{423.15K}$
K	MPa	MPa	kg·m^{-3}	kg·m^{-3}	μPa·s	μPa·s
423.093	0.079423	0.079366	0.99883	0.99969	11.354[a]	11.356[a]
423.089	0.15842	0.15825	1.9998	2.0023	11.369	11.370
423.086	0.31359	0.31356	3.9954	3.9964	11.396	11.398
423.083	0.46701	0.46692	5.9988	6.0011	11.421	11.423
423.080	0.46702	0.46703	6.0003	6.0012	11.425	11.427
423.084	0.61143	0.61120	7.9148	7.9192	11.449	11.451
423.077	0.61167	0.61147	7.9184	7.9226	11.449	11.451
423.084	0.76355	0.76344	9.9704	9.9736	11.478	11.480
423.083	0.76373	0.76361	9.9726	9.9761	11.480	11.482
423.084	0.92077	0.92080	12.133	12.135	11.513	11.514
423.079	0.92089	0.92080	12.133	12.137	11.514	11.516
423.094	1.0601	1.0602	14.082	14.083	11.551	11.552
423.097	1.0612	1.0613	14.098	14.099	11.551	11.553
423.092	1.1924	1.1927	15.966	15.964	11.581	11.582
423.093	1.1932	1.1935	15.977	15.975	11.581	11.582
423.099	1.3344	1.3347	18.018	18.016	11.624	11.625
423.100	1.3355	1.3357	18.032	18.032	11.622	11.623
423.097	1.4545	1.4548	19.782	19.780	11.658	11.660
423.100	1.4545	1.4548	19.781	19.780	11.657	11.658
423.086	2.1093	2.1100	29.905	29.900	11.888	11.890
423.080	2.1099	2.1107	29.916	29.911	11.886	11.888
423.081	2.7034	2.7043	39.922	39.918	12.167	12.168
423.076	2.7038	2.7048	39.931	39.926	12.165	12.167
423.095	3.2417	3.2426	49.821	49.816	12.476	12.477
423.097	3.2423	3.2433	49.834	49.827	12.476	12.478
423.072	3.7464	3.7479	59.965	59.957	12.833	12.835
423.061	3.7473	3.7492	59.991	59.979	12.835	12.838
423.073	4.2057	4.2074	70.041	70.033	13.230	13.232
423.065	4.2060	4.2079	70.052	70.043	13.227	13.229
423.087	4.6153	4.6167	79.819	79.816	13.647	13.649
423.090	4.6159	4.6173	79.834	79.829	13.650	13.651
423.057	5.0050	5.0075	89.970	89.965	14.122	14.125
423.044	5.0058	5.0086	90.002	89.996	14.121	14.124
423.056	5.3559	5.3586	99.870	99.866	14.618	14.621
423.043	5.3572	5.3602	99.917	99.915	14.620	14.622
423.072	5.9870	5.9898	119.769	119.768	15.730	15.732
423.081	5.9870	5.9895	119.759	119.757	15.731	15.732
423.075	6.5415	6.5451	139.717	139.703	16.996	16.998
423.080	6.5419	6.5453	139.725	139.710	16.999	17.000
423.097	7.0292	7.0330	159.017	158.975	18.380	18.381
423.098	7.0300	7.0337	159.048	159.005	18.379	18.381
423.097	7.5150	7.5201	179.397	179.315	20.022	20.023
423.103	7.5159	7.5208	179.425	179.338	20.019	20.020
423.081	7.9847	7.9922	199.277	199.167	21.823	21.824
423.082	7.9851	7.9926	199.294	199.181	21.823	21.825
423.041	8.5042	8.5164	220.267	220.140	23.942	23.945
423.058	8.5051	8.5160	220.253	220.121	23.952	23.954
423.044	9.0662	9.0799	240.492	240.364	26.229	26.232
423.058	9.0673	9.0796	240.483	240.357	26.239	26.241
423.049	9.7245	9.7385	260.612	260.521	28.776	28.779
423.061	9.7257	9.7384	260.609	260.519	28.771	28.773
423.038	10.527	10.544	280.644	280.573	31.596	31.599

Table 10. Continued

T	p	$p_{423.15K,\rho_{exp}}$	ρ_{exp}	$\rho_{eos(T,p)}$	η	$\eta_{423.15K}$
K	MPa	MPa	kg·m^{-3}	kg·m^{-3}	μPa·s	μPa·s
423.048	10.528	10.543	280.635	280.568	31.603	31.605
423.040	11.547	11.566	300.645	300.589	34.764	34.767
423.050	11.549	11.566	300.654	300.599	34.763	34.766
423.096	12.871	12.882	320.474	320.437	38.266	38.267
423.098	12.872	12.884	320.488	320.446	38.282	38.283
423.084	14.679	14.693	341.059	341.037	42.354	42.355
423.089	14.680	14.693	341.059	341.038	42.342	42.344
423.044	17.040	17.065	361.234	361.216	46.909	46.911
423.058	17.043	17.064	361.230	361.216	46.935	46.937
423.042	20.165	20.193	381.229	381.222	52.086	52.089
423.056	20.168	20.192	381.227	381.219	52.088	52.090
423.055	24.305	24.333	401.231	401.226	57.981	57.983
423.064	24.308	24.334	401.235	401.228	57.949	57.951
423.094	29.682	29.700	421.002	421.002	64.635	64.637
423.096	29.685	29.703	421.011	421.010	64.660	64.662

[a] Influenced by slip.

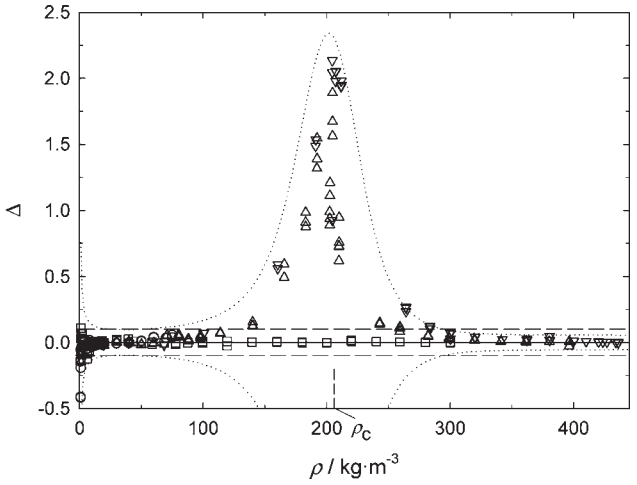

Figure 5. Comparison of the experimental density data for ethane with values calculated for the equation of state by Bücker and Wagner[1] using the measured temperatures and pressures as a function of density ρ. Deviations: $\Delta = 100(\rho_{exp} - \rho_{eos})/\rho_{eos}$. ○, 298.15 K for ethane 3.5; △, 307.15 K for ethane 3.5; ▽, 307.15 K for ethane 5.0; □, 423.15 K for ethane 5.0; — — —, uncertainty ± 0.1 %; · · ·, total uncertainty in the density measurement (eq 1) for ethane at 307.15 K.

isotherm at 373.15 K, the deviations are increased to +1.2 %, whereas the maximum total uncertainty of experimental $p\rho T$ data could come up to ± 1.49 % for this isotherm as estimated above. In Figure 8, the experimentally obtained pressures are compared to values calculated for the equation of state by Lemmon et al. using the experimental temperatures and densities. It is obvious that an uncertainty in pressure of ± 0.05 % is exceeded in the low-density range as well as at densities larger than the critical density (ρ_c = 220.48 kg·m^{-3}) for the isotherm at 373.15 K. This could possibly be due to larger uncertainties in the density measurement at high pressures.

Viscosity. The experimental results of each nominal isotherm for ethane and propane were correlated as a function of the reduced density δ by means of a power-series representation

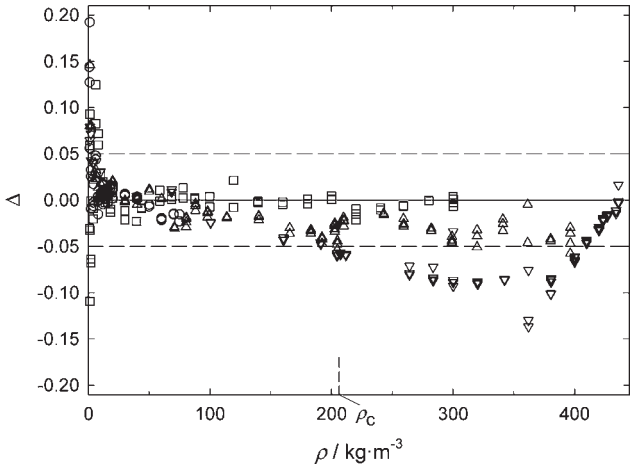

Figure 6. Comparison of the measured pressures for ethane with values calculated for the equation of state by Bücker and Wagner[1] using the measured temperatures and densities as a function of density ρ. Deviations: $\Delta = 100(p_{exp} - p_{eos})/p_{eos}$. ○, 298.15 K for ethane 3.5; △, 307.15 K for ethane 3.5; ▽, 307.15 K for ethane 5.0; □, 423.15 K for ethane 5.0.

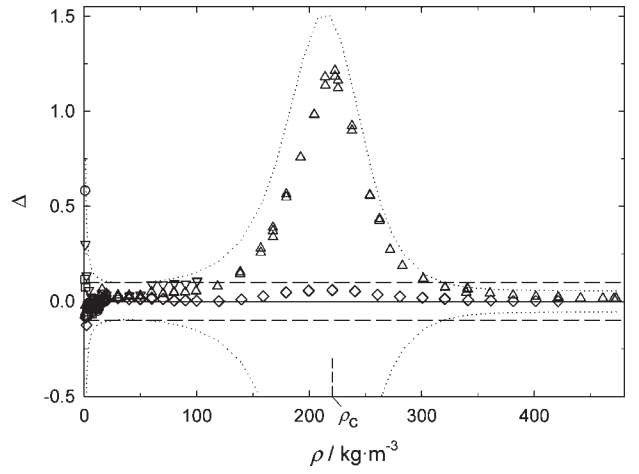

Figure 7. Comparison of the measured densities for propane with values calculated for the equation of state by Lemmon et al.[2] using the measured temperatures and pressures as a function of density ρ. Deviations: $\Delta = 100(\rho_{exp} - \rho_{eos})/\rho_{eos}$. □, 273.15 K; ○, 298.15 K; ▽, 366.15 K; △, 373.15 K; ◇, 423.15 K; − − −, uncertainty ± 0.1 %; ···, total uncertainty in the density measurement (eq 1) for propane at 373.15 K.

restricted to the sixth or a lower power depending on the density range and on the reduced temperature τ:

$$\eta(\tau,\delta) = \sum_{i=0}^{n} \eta_i(\tau)\delta^i \qquad \delta = \frac{\rho}{\rho_{c,fluid}} \qquad \tau = \frac{T}{T_{c,fluid}} \qquad (4)$$

$$\text{with } T_{c,C_2H_6} = 305.322 \text{ K}, \; T_{c,C_3H_8} = 369.89 \text{ K},$$
$$\rho_{c,C_2H_6} = 206.18 \text{ kg·m}^{-3}, \; \rho_{c,C_3H_8} = 220.48 \text{ kg·m}^{-3}$$

The values of the critical temperatures $T_{c,fluid}$ and critical densities $\rho_{c,fluid}$ are those given by Bücker and Wagner[1] and by Lemmon et al.[2] Weighting factors of η_{exp}^{-2} were used in the multiple linear least-squares regression to minimize the relative

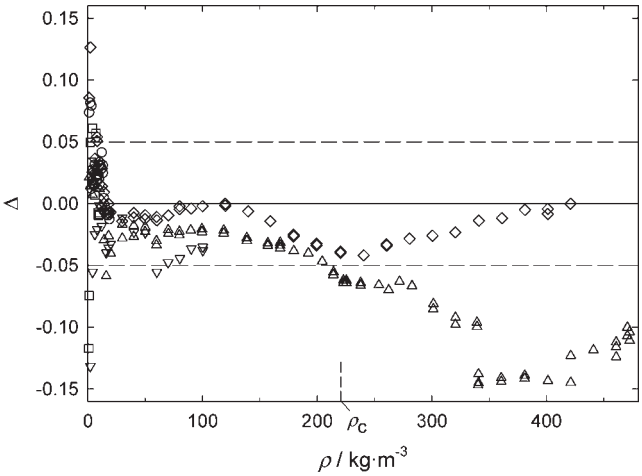

Figure 8. Comparison of the measured pressures for propane with values calculated for the equation of state by Lemmon et al.[2] using the measured temperatures and densities as a function of density ρ. Deviations: $\Delta = 100(p_{exp} - p_{eos})/p_{eos}$. □, 273.15 K; ○, 298.15 K; ▽, 366.15 K; △, 373.15 K; ◇, 423.15 K.

deviations for the different isotherms. The weighted standard deviation was employed as criterion for the quality of the representation of the considered isotherm. The coefficients $\eta_i(\tau)$ of eq 4 including their standard deviations SD_{η_i} and the weighted standard deviation σ are given in Table 11 for ethane and propane. Furthermore, the corresponding information resulting from the re-evaluated data for ethane by Wilhelm et al.[9] and for propane by Wilhelm and Vogel[10] has been listed in the correction reports.[11,12]

Ethane. The effect of the critical enhancement of the viscosity in the extended critical region is demonstrated by means of Figure 9 for the measurements of the nominal isotherm at 307.15 K. At first it was found that a usual power-series expansion of sixth order was not suitable to describe all of the viscosity data of this isotherm in an appropriate manner, particularly those in the density range of $0.80 \le \delta = (\rho/\rho_c) \le 1.26$. Therefore, these data were excluded from the correlation with the power series. As shown in the figure, the excluded viscosity values differ by maxima of +1.7 % and of +2.2 % from the power series for the ethane 3.5 and 5.0 samples. The maximum differences occur near the critical density. The experimental data considered for the power-series expansion agree within ± 0.1 % with the fitted values.

The experimental viscosity data of this paper are compared with values calculated for the viscosity surface correlation of Hendl et al.[3] using the measured values for temperature and density. This correlation is characterized by uncertainties of ± 2.5 % in the vapor phase at subcritical temperatures down to 250 K, of ± 2.5 % at supercritical temperatures to 500 K and for pressures to 60 MPa, and of ± 3 % at higher supercritical temperatures to 1000 K and for pressures of (1 to 3) MPa. It is to note that the correlation of Hendl et al. includes a contribution for the viscosity in the limit of zero density (see also Hendl et al.[27]) as well as another one considering the critical enhancement of viscosity. The comparison between the experimental data of this paper and the complete viscosity surface correlation by Hendl et al. is illustrated in Figure 10. In addition, deviations between the experimental data and values calculated for the correlation without the critical-enhancement contribution are

Table 11. Coefficients of Equation 4 for the Viscosity Measurements on Ethane and Propane

	T		ρ_{max}	η_0	η_1	η_2	η_3
sample	K	n	kg·m^{-3}	μPa·s	μPa·s	μPa·s	μPa·s
ethane 3.5	293.15	3	74.95	9.068 ± 0.001	1.380 ± 0.017	11.721 ± 0.131	−4.048 ± 0.261
ethane 3.5	307.15	6	396.60	9.476 ± 0.002	3.017 ± 0.052	6.299 ± 0.323	7.088 ± 0.799
ethane 5.0	307.15	6	436.19	9.503 ± 0.003	3.012 ± 0.071	7.359 ± 0.418	4.480 ± 0.970
ethane 5.0	423.15	4	300.20	12.768 ± 0.001	3.761 ± 0.022	9.543 ± 0.076	−3.296 ± 0.088

T	η_4	η_5	η_6	
K	μPa·s	μPa·s	μPa·s	σ
293.15				0.017
307.15	−7.462 ± 0.882	3.279 ± 0.442	−0.306 ± 0.082	0.053
307.15	−4.882 ± 0.991	2.106 ± 0.451	−0.106 ± 0.075	0.051
423.15	2.063 ± 0.032			0.026

	T		ρ_{max}	η_0	η_1	η_2	η_3
sample	K	n	kg·m^{-3}	μPa·s	μPa·s	μPa·s	μPa·s
propane 3.5	273.15	2	9.98	7.457 ± 0.001	−1.707 ± 0.113	11.562 ± 1.967	
propane 3.5	298.15	2	18.65	8.135 ± 0.001	−0.695 ± 0.063	10.980 ± 0.679	
propane 3.5	366.15	4	100.27	9.914 ± 0.002	1.132 ± 0.063	15.295 ± 0.604	−14.392 ± 2.080
propane 3.5	373.15	6	472.62	10.096 ± 0.007	1.476 ± 0.140	16.528 ± 0.747	−15.639 ± 1.578
propane 3.5	423.15	6	421.01	11.351 ± 0.001	2.279 ± 0.031	13.799 ± 0.177	−10.311 ± 0.413

T	η_4	η_5	η_6	
K	μPa·s	μPa·s	μPa·s	σ
273.15				0.010
298.15				0.021
366.15	13.612 ± 2.303			0.020
373.15	15.838 ± 1.528	−7.203 ± 0.685	1.471 ± 0.115	0.111
423.15	10.631 ± 0.450	−4.870 ± 0.228	1.088 ± 0.043	0.022

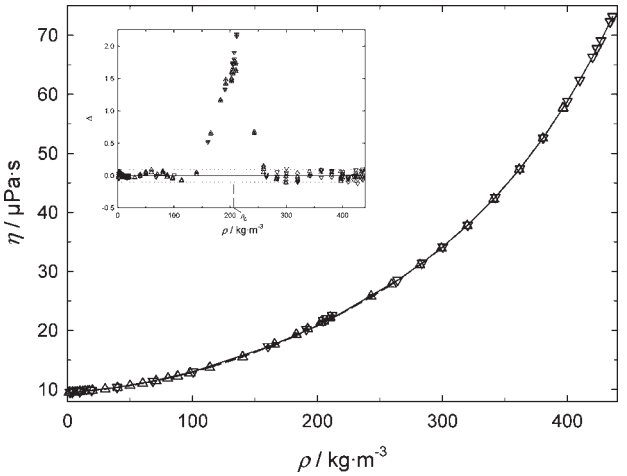

Figure 9. Viscosity of ethane at 307.15 K as a function of density ρ. △, measured data for ethane 3.5; ▽, measured data for ethane 5.0; △ with cross, measured data for ethane 3.5 influenced by the critical enhancement; ▽ with cross, measured data for ethane 5.0 influenced by the critical enhancement; —, ethane 3.5, — — —, ethane 5.0, each fitted with a power series expansion of sixth order in the reduced density δ (eq 4, Table 11). Deviations in inset: $\Delta = 100(\eta_{exp} - \eta_{fit})/\eta_{fit}$.

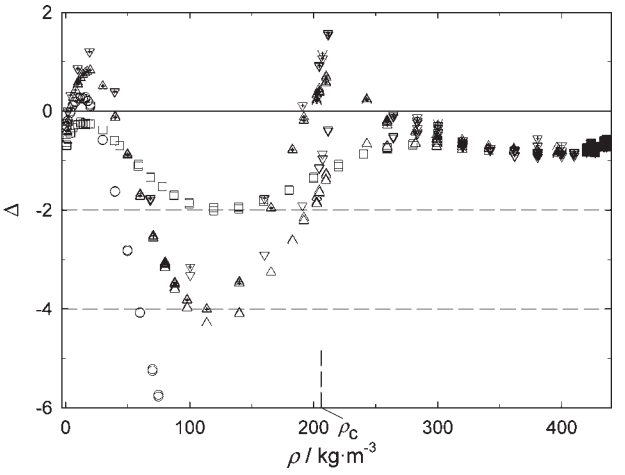

Figure 10. Comparison of experimental viscosity data for ethane with calculated values using the correlation by Hendl et al.[3] and measured values for temperature and density. Deviations: $\Delta = 100(\eta_{exp} - \eta_{cor})/\eta_{cor}$. ○, 293.15 K for ethane 3.5; △, 307.15 K for ethane 3.5; △ with cross, 307.15 K for ethane 3.5, correlation without critical enhancement; ▽, 307.15 K for ethane 5.0; ▽ with cross, 307.15 K for ethane 5.0, correlation without critical enhancement; □, 423.15 K for ethane 5.0.

dx.doi.org/10.1021/je101178u |J. Chem. Eng. Data 2011, 56, 1476–1493

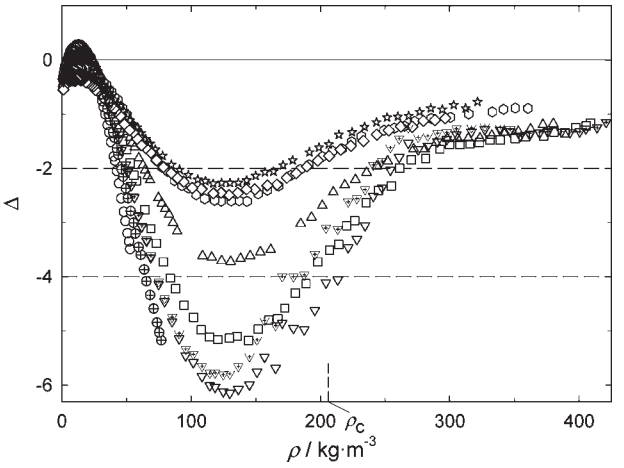

Figure 11. Comparison of re-evaluated experimental viscosity data of Wilhelm et al.[11] for ethane with calculated values, using the correlation by Hendl et al.[3] and measured values for temperature and calculated values for density. Deviations: $\Delta = 100(\eta_{exp} - \eta_{cor})/\eta_{cor}$. ○, 290 K; ⊕, 300 K; ▽, 310 K; ▽ with cross, 310 K, correlation without critical enhancement; □, 320 K; △, 340 K; ⬡, 370 K; ☆, 400 K; ◇, 430 K.

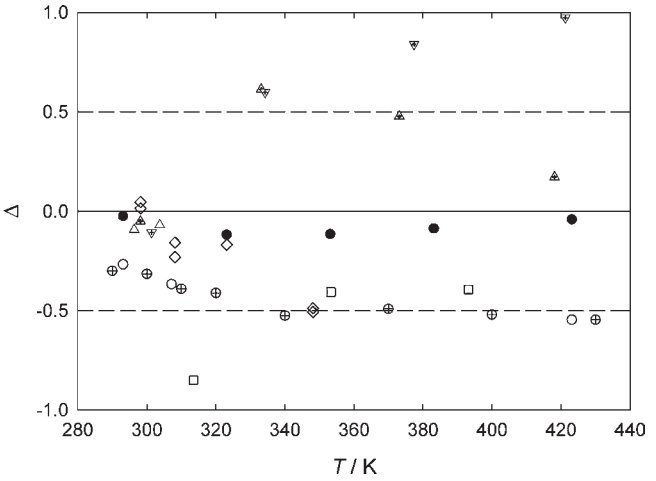

Figure 12. Comparison of reliable experimental data for ethane at low densities with calculated values of the correlation by Hendl et al.[3] as a function of temperature T. Deviations: $\Delta = 100(\eta_{exp} - \eta_{cor})/\eta_{cor}$. △, Kestin et al.;[31] ▽ with cross, Kestin et al.;[32] △ with cross, Abe et al.;[33] ◇, Iwasaki and Takahashi;[34] □, Hunter and Smith;[35] ●, Hendl and Vogel;[17] ⊕, Wilhelm et al.;[11] ○, this work.

shown for the two measurement series of the isotherm at 307.15 K. The figure makes evident that the critical enhancement has to be taken into account. Without this contribution an awkward maximum occurs in the course of the deviations when approaching the critical density. The contribution of the critical enhancement amounts to about 2 % near to the critical density and reduces to approximately 0.2 % at 100 kg·m^{-3} and 300 kg·m^{-3}. Furthermore, Figure 10 shows maximum deviations of −5.7 % for the subcritical isotherm at 293.15 K, of −4.2 % for the near-critical isotherm at 307.15 K, and of −2.0 % for the supercritical isotherm at 423.15 K. The deviations for the two lower isotherms exceed the uncertainty of the viscosity surface correlation of Hendl et al.[3] On the other hand, the experimental data of this paper are on average only 1 % lower than the values of the correlation in the range of densities > 230 kg·m^{-3}.

The re-evaluated viscosity data by Wilhelm et al.[9] presented in the correction report[11] are compared in Figure 11 with the viscosity surface correlation of Hendl et al.[3] using the measured values for temperature and the calculated values for density. The figure makes obvious that the deviations between the experimental data and the correlation are still somewhat larger, such as about 2 % more for the isotherm at 310 K of the re-evaluated viscosity data by Wilhelm et al. compared with those for the isotherm at 307.15 K of this paper. Here it is taken into account that the isotherm at 310 K is another 2.85 K away from the critical temperature. Although the density was not directly measured by Wilhelm et al., it is again to note that the deviations from the correlation are distinctly larger than its estimated uncertainty. This concerns widely the experimental data of the isotherms of $T \leq 340$ K at densities of $(50 < \rho < 200)$ kg·m^{-3}.

Moreover, at low densities near to atmospheric pressure, a comparison of selected reliable experimental data from the literature, of the present data, and of the re-evaluated data by Wilhelm et al.[11] with values calculated for the viscosity surface correlation by Hendl et al.[3] is given in Figure 12. The figure shows that most of the data agree in the considered temperature range within ± 0.5 % with the correlation by Hendl et al.[3] and hence with its zero-density contribution first reported by Hendl et al.[27] In this context the viscosity values at room temperature have to be discussed primarily, since most measurements are relative and based on a calibration with rare gases at this temperature. The theoretically calculated values, for helium by Bich et al.[13] used for the present measurements and for argon by Vogel et al.[19] used for the re-evaluation of the data by Wilhelm et al.,[9] differ by about −0.2 % from the values by Kestin and Leidenfrost[28] and by Kestin et al.[29,30] which were often used for the calibration in earlier measurements. This explains that the low-density viscosity data of the present paper at 293.15 K and the re-evaluated data by Wilhelm et al.[11] at (290 and 300) K, shown in Figure 12, deviate by −(0.25 to 0.3) % from the values calculated for the correlation by Hendl et al.[3] and from the experimental room-temperature datum by Hendl and Vogel[17] which belongs to the primary experimental database of the correlation by Hendl et al. For that reason, there exists an excellent agreement between the experimental data of Hendl and Vogel[17] and the viscosity correlation of Hendl et al. in the complete temperature range. Apart from the data by Hunter and Smith[35] which were determined with an uncertainty of ± (0.75 to 1.25) % using a capillary viscometer, the other data measured with oscillating-disk viscometers by Kestin and coworkers[31−33] and by Iwasaki and Takahashi[34] agree perfectly at room temperature. But the data by Kestin et al.[32] and Abe et al.[33] deviate distinctly at higher temperatures, whereas the temperature function of the viscosity values measured with the vibrating-wire viscometers of Wilhelm et al.[11] and of this work is in close agreement with that of the data by Hendl and Vogel[17] obtained with an oscillating-disk viscometer. In this regard it is to state that the measurements by Kestin and coworkers[32,33] are influenced by a temperature measurement error discussed extensively by Vogel et al.[36]

Propane. The evaluation of the series of viscosity measurements for the nominal isotherm at 373.15 K showed that a usual power-series expansion of sixth order was not adequate to represent the viscosity data of this isotherm in an appropriate manner. For that reason the viscosity data from the density range of $0.88 \leq \delta \leq 1.24$ were excluded from the fit of the power-series expansion. Figure 13 makes obvious that these viscosity data

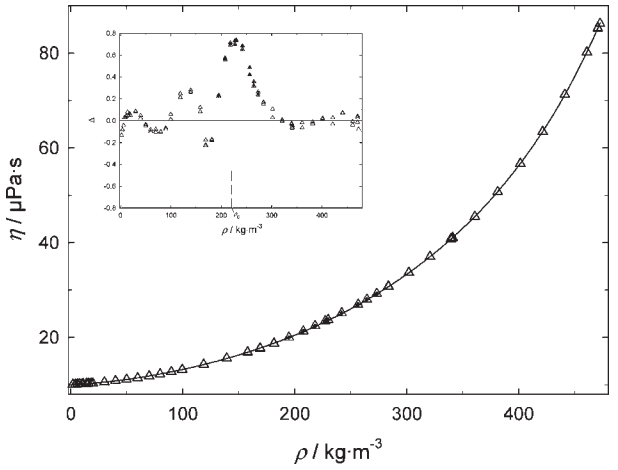

Figure 13. Viscosity of propane at 373.15 K as a function of density ρ. △, measured data; △ with cross, measured data influenced by the critical enhancement; —, fitted with a power series expansion of sixth order in the reduced density δ (eq 4, Table 11). Deviations in inset: $\Delta = 100(\eta_{exp} - \eta_{fit})/\eta_{fit}$.

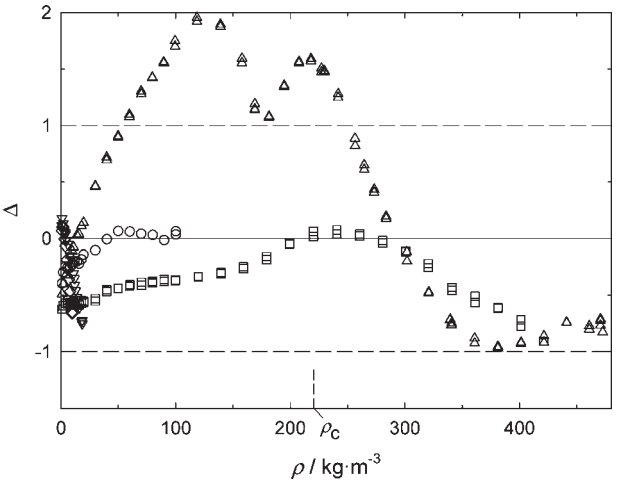

Figure 14. Comparison of experimental viscosity data for propane with calculated values using the correlation by Scalabrin et al.[4] and measured values for temperature and density. Deviations: $\Delta = 100(\eta_{exp} - \eta_{cor})/\eta_{cor}$. ◇, 273.15 K; ▽, 298.15 K; ○, 366.15 K; △, 373.15 K; □, 423.15 K.

differ maximal by +0.74 % from the fitted values at densities near the critical one, in accordance with the expected positive differences due to the enhancement of viscosity in the extended critical region. But the figure shows also a woven distribution of the deviations between $-0.23 < \Delta/\% < +0.28$ in the density range $100 < \rho/kg \cdot m^{-3} < 180$. A possible cause for this state of affairs could consist in a failure of the viscosity measurement due to convection along the vibrating wire, as marked in Table 9. But the resulting viscosity data are still of high quality.

The experimental viscosity data of this paper are compared with values calculated for the viscosity surface correlation of Scalabrin et al.[4] using the measured values for temperature and density. This correlation is a multiparameter viscosity equation developed using the optimization technique by Setzmann and Wagner.[37] Starting from a bank of terms, the optimization algorithm determines the functional form of the equation in a way that the best description of the selected primary data is obtained. The correlation by Scalabrin et al. represents a significant improvement compared with the former reference correlation by Vogel et al.,[36] particularly because it could be based on the more recent extensive viscosity measurements by Wilhelm and Vogel[10] in the vapor phase and in the supercritical region. Furthermore, Scalabrin et al. could use a more accurate equation of state to convert the independent variables temperature T and pressure p, used in most measurements of the literature, into the independent variables temperature T and density ρ, needed for the viscosity correlation. Whereas Vogel et al. applied the modified Benedict−Webb−Rubin equation of state by Younglove and Ely,[38] Scalabrin et al. based their correlation on the equation of state by Span and Wagner.[20] As a final result, Scalabrin et al. represented the selected 1024 primary data points with an average absolute deviation of 0.28 % and defined the validity range of their correlation to be the liquid phase for temperatures $90 < T/K < 370$ and pressures ≤ 100 MPa as well as the vapor and supercritical regions for temperatures $210 < T/K < 625$ and pressures ≤ 100 MPa.

Some further remarks are essential with regard to the comparison with the viscosity surface correlation of Scalabrin et al.[4] This correlation does not include any contribution for the critical enhancement of viscosity, although Wilhelm and Vogel[10] performed a series of measurements at 373.15 K, that means a near-critical isotherm. But as already mentioned, the needed densities for these measurements were obtained from measured temperatures and pressures so that large uncertainties for the densities and also for the viscosities had to be expected. Hence Scalabrin et al. found for this series at 373.15 K large deviations from the surface correlation increasing to −4.4 % when approaching the critical density. Nevertheless, any effect of the critical enhancement of viscosity could possibly had been hidden in the results of these measurements.

In addition, Scalabrin et al.[4] regretted that no experimental data are available in the vapor phase for $T < 292$ K and stated that no viscosity minima became evident at those temperatures for which data were available. But the measurements of Vogel[18] and of Wilhelm and Vogel[10] had already yielded negative values for the initial density viscosity coefficient η_1 and revealed consequently viscosity minima. The uncertainty of these measurements is very low so that there is no doubt in these results. In particular, the series of measurements at 298.15 K of Wilhelm and Vogel shows clearly a minimum. In this context it is to note that the correlations by Vogel et al.[36] and by Scalabrin et al. differ in the treatment of the zero-density and initial-density viscosity coefficients. Whereas Vogel et al. used a theoretical background for the analysis of the low-density contributions, Scalabrin et al. did not feature specifically them in their analysis for the complete viscosity surface correlation. The number of terms of their surface correlation representing the low-density region is obviously not high enough to describe adequately these high-precision measurements. Since Scalabrin et al. were conscious of that problem, they analyzed separately the measurements of Wilhelm and Vogel[10] up to densities of 4.41 $kg \cdot m^{-3}$ and those of Vogel[18] and derived a distinctly better representation of the data, but using an increased number of terms (see eqs 11 to 13 of that paper).

The comparison between the experimental data of this paper and the complete viscosity surface correlation by Scalabrin et al.[4] is illustrated in Figure 14. Taking into account that a new viscosity standard (0.2 % lower) was used for the calibration of the viscometer at room temperature and at zero density, the new

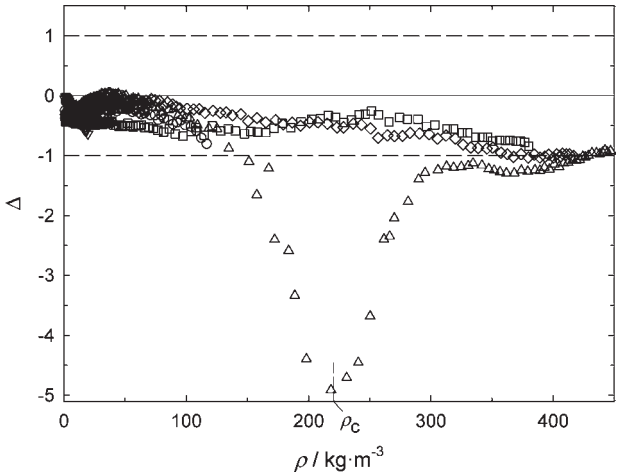

Figure 15. Comparison of re-evaluated experimental viscosity data of Wilhelm and Vogel[12] for propane with calculated values, using the correlation by Scalabrin et al.[4] and measured values for temperature and calculated values for density. Deviations: $\Delta = 100(\eta_{exp} - \eta_{cor})/\eta_{cor}$. ▽, 298.15 K; ⊕, 323.15 K; ⬡, 348.15 K; ○, 366.15 K; △, 373.15 K; ◇, 398.15 K; □, 423.15 K.

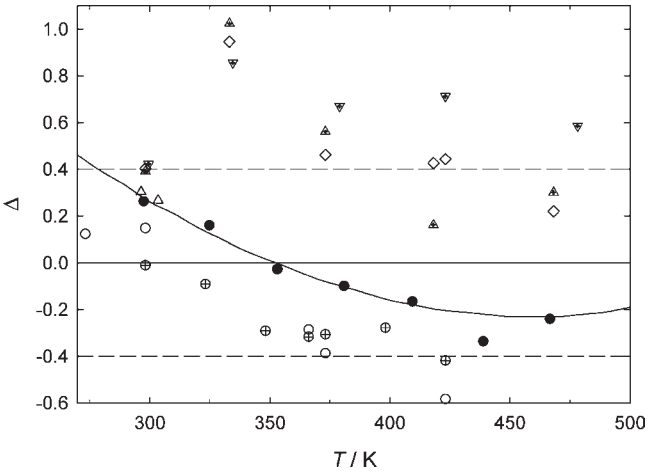

Figure 16. Comparison of reliable experimental data for propane at low densities with calculated values of the correlation by Scalabrin et al.[4] as a function of temperature T. Deviations: $\Delta = 100(\eta_{exp} - \eta_{cor})/\eta_{cor}$. —, special correlation for low-density gas (eqs 11 to 13 of that paper) by Scalabrin et al.;[4] △, Kestin et al.;[31] ▽ with cross, Kestin et al.;[32] △ with cross, Abe et al.;[33] ◇, Abe et al.;[39] ●, Vogel (series 3 of measurements);[18] ⊕, Wilhelm and Vogel;[12] ○, this work.

experimental data deviate only within ± 0.5 % from the surface correlation by Scalabrin et al. for all temperatures in the range of moderate densities to about 20 kg·m^{-3}. For the subcritical isotherm at 366.15 K extending to densities of 100 kg·m^{-3} and for the supercritical isotherm at 423.15 K in the complete density range, the deviations do not exceed ± 0.7 %. For the isotherm at 373.15 K, large deviations to +2.2 % appear at densities in the range of 120 < ρ/kg·m^{-3} < 140. Although the differences decrease with increasing density, a hump up to +1.8 % occurs near the critical density indicating the critical enhancement which had to be expected according to the analysis with the power-series expansion (compare Figure 13 and its discussion).

The re-evaluated viscosity data by Wilhelm and Vogel[10] presented in the correction report[12] are compared in Figure 15 with the viscosity surface correlation of Scalabrin et al.[4] using the measured values for temperature and the calculated values for density. The figure makes evident that the corrected experimental data deviate from the surface correlation by maximum −1 % in the complete density range for all isotherms apart from the near-critical one at 373.15 K. These deviations enlarge to about −5 % when approaching the critical density. Considering the experimental data of this paper (see Figure 14), it is to conclude that the viscosity data by Wilhelm and Vogel of this isotherm are strongly influenced by the uncertainty of the density determination from measured temperatures and pressures. Hence Scalabrin et al. were right to give these data low weights in their analysis.

Moreover, at low densities near to atmospheric pressure, a comparison of selected experimental data from the literature, of the present data, and of the re-evaluated data by Wilhelm and Vogel[12] with values calculated for the complete viscosity surface correlation by Scalabrin et al.[4] is given in Figure 16. The low-density gas correlation by Scalabrin et al., mentioned above and additionally plotted in this figure, elucidates the better representation of the experimental data by Vogel[18] as well as of those by Wilhelm and Vogel[12] and of those of the present paper. Here it is to take into account that the data of the last two papers are based on an improved calibration of the viscometers. At higher temperatures the data by Kestin et al.[32] and by Abe et al.[33,39] deviate distinctly once again from the low-density gas correlation by Scalabrin et al., for the same reason as in the case of ethane.

CONCLUSIONS

A newly designed apparatus combining a vibrating-wire viscometer and a single-sinker densimeter was used to perform quasi-simultaneous measurements of viscosity and density on gaseous ethane and propane. The density determination is characterized by a relative uncertainty of lower than ± 0.1 % for densities ρ > 15 kg·m^{-3}. For the near-critical isotherms at 307.15 K for ethane and at 373.15 K for propane, the allocation errors for temperature and pressure increase the maximum total uncertainty of the experimental $p\rho T$ data to ± 2.35 % and ± 1.49 %, respectively. The general uncertainty in the density data leads to an uncertainty in viscosity of about ± (0.25 to 0.3) %, only increased by 0.04 % in the near-critical region of the fluids due to the allocation errors arising from the temperature and density measurements.

The density data were compared with values calculated using the experimentally obtained values for pressure and temperature as well as reference equations of state, for ethane by Bücker and Wagner[1] and for propane by Lemmon et al.[2] The deviations in density from the equations of state are within ± 0.1 %, excluding the low-density and the near-critical regions. But the isotherms at 307.15 K for ethane and at 373.15 K for propane reveal differences of +2.1 % and to +1.2 %, respectively. When comparing the values for the pressure, deviations of ± 0.05 % occur except for lower densities and experimental points of the near-critical isotherms.

The results of re-evaluated earlier viscosity measurements of our group on ethane by Wilhelm et al.[9] and on propane by Wilhelm and Vogel[10] reported in separate corrections[11,12] were included in this paper. The re-evaluation concerns a recalibration using an improved value calculated theoretically for the zero-density viscosity coefficient of argon at room temperature. Besides this, the density values for propane needed for the viscosity determination by Wilhelm and Vogel were recalculated using the new equation of state by Lemmon et al.[2] Since the densities for

the re-evaluation had to be taken from an equation of state, for ethane from that of Bücker and Wagner,[1] instead of measuring it simultaneously, larger deviations from the new viscosity data are expected in the near-critical region.

The new viscosity data of this paper and the re-evaluated data by Wilhelm et al.[11] for ethane and by Wilhelm and Vogel[12] for propane were compared with viscosity surface correlations by Hendl et al.[3] for ethane and by Scalabrin et al.[4] for propane as well as with selected experimental data for the low-density region available in the literature. For ethane, the maximum deviations of the new data exceed the stated uncertainty of ± 2.5 % for the viscosity surface correlation at 293.15 K (−5.7 %) and at 307.15 K (−4.2 %), whereas the average deviation from the correlation attains only about −1 % for densities > 230 $kg \cdot m^{-3}$. Similar deviations occur for the re-evaluated data. In the low-density region, the room temperature values and the temperature functions of the new and of the re-evaluated experimental data for ethane are in close agreement to the viscosity values of the surface correlation. For propane, the deviations of the new experimental data from the surface correlation, which considers the original data by Wilhelm and Vogel,[10] do not exceed ± 0.7 % (maximum −1 %) for all temperatures in the complete density range, except for the near-critical isotherm at 373.15 K. The re-evaluated viscosity data by Wilhelm and Vogel[12] do not differ more than −1 % from the correlation, again except for the near-critical isotherm. The low-density gas contribution of the complete viscosity surface contribution by Scalabrin et al. could a little be improved to represent the experimental data by Vogel[18] and the re-evaluated values by Wilhelm and Vogel[12] as well as those of the present paper within their low uncertainties.

The effect of the critical enhancement of the viscosity in the extended critical region became evident for the near-critical isotherms, for ethane at 307.15 K and for propane at 373.15 K. For ethane the contribution of the critical enhancement amounts to about 2 % near the critical density, conforming to the viscosity surface correlation by Hendl et al.[3] For propane it achieves +0.74 %, considering that the isotherm is by 1.43 K farther from the critical temperature. Since the viscosity surface correlation by Scalabrin et al.[4] did not include a critical enhancement contribution, larger differences up to +1.6 % occur for this isotherm near the critical density.

As a result of the investigations, the new viscosity data of this paper as well as the re-evaluated values by Wilhelm et al.[11] and Wilhelm and Vogel[12] are appropriate to diminish the uncertainty of viscosity surface correlations for these fluids. When generating new correlations, the low-density region and the critical enhancement in the near-critical region should be considered by using adequate models.

AUTHOR INFORMATION

Corresponding Author

*E-mail: eckhard.vogel@uni-rostock.de.

Funding Sources

This work was financially supported by the German Science Foundation (Deutsche Forschungsgemeinschaft), Grant No. VO 499/11-1 and -2.

REFERENCES

(1) Bücker, D.; Wagner, W. A Reference Equation of State for the Thermodynamic Properties of Ethane for Temperatures from the Melting Line to 675 K and Pressures up to 900 MPa. *J. Phys. Chem. Ref. Data* **2006**, *35*, 205–266.

(2) Lemmon, E. W.; McLinden, M. O.; Wagner, W. Thermodynamic Properties of Propane. III. A Reference Equation of State for Temperatures from the Melting Line to 650 K and Pressures up to 1000 MPa. *J. Chem. Eng. Data* **2009**, *54*, 3141–3180.

(3) Hendl, S.; Millat, J.; Vogel, E.; Vesovic, V.; Wakeham, W. A.; Luettmer-Strathmann, J.; Sengers, J. V.; Assael, M. J. The Transport Properties of Ethane. I. Viscosity. *Int. J. Thermophys.* **1994**, *15*, 1–31.

(4) Scalabrin, G.; Marchi, P.; Span, R. A Reference Multiparameter Viscosity Equation for Propane with an Optimized Functional Form. *J. Phys. Chem. Ref. Data* **2006**, *35*, 1415–1442.

(5) Seibt, D.; Herrmann, S.; Vogel, E.; Bich, E.; Hassel, E. Simultaneous Measurements on Helium and Nitrogen with a Newly Designed Viscometer-Densimeter over a Wide Range of Temperature and Pressure. *J. Chem. Eng. Data* **2009**, *54*, 2626–2637.

(6) Wilhelm, J.; Vogel, E.; Lehmann, J. K.; Wakeham, W. A. A Vibrating-Wire Viscometer for Dilute and Dense Gases. *Int. J. Thermophys.* **1998**, *19*, 391–401.

(7) Wilhelm, J.; Vogel, E. Viscosity Measurements on Gaseous Argon, Krypton, and Propane. *Int. J. Thermophys.* **2000**, *21*, 301–318.

(8) Seibt, D. Schwingdrahtviskosimeter mit integriertem Ein-Senkkörper-Dichtemessverfahren für Untersuchungen an Gasen in größeren Temperatur- und Druckbereichen. *Fortschr.-Ber. VDI, Reihe 6: Energietechnik*; VDI-Verlag: Düsseldorf, 2008; Nr. 571.

(9) Wilhelm, J.; Seibt, D.; Vogel, E.; Buttig, D.; Hassel, E. Viscosity Measurements on Gaseous Ethane. *J. Chem. Eng. Data* **2006**, *51* 136–144.

(10) Wilhelm, J.; Vogel, E. Viscosity Measurements on Gaseous Propane. *J. Chem. Eng. Data* **2001**, *46*, 1467–1471.

(11) Wilhelm, J.; Seibt, D.; Vogel, E.; Buttig, D.; Hassel, E. *J. Chem. Eng. Data* **2006**, *51*, 136–144. Wilhelm, J.; Seibt, D.; Vogel, E.; Buttig, D.; Hassel, E. Viscosity Measurements on Gaseous Ethane: Re-evaluation. *J. Chem. Eng. Data* **2011**, in press.

(12) Wilhelm, J.; Vogel, E. Viscosity Measurements on Gaseous Propane. *J. Chem. Eng. Data* **2001**, *46*, 1467–1471. Wilhelm, J.; Vogel, E. Viscosity Measurements on Gaseous Propane: Re-evaluation. *J. Chem. Eng. Data* **2011**, in press.

(13) Bich, E.; Hellmann, R.; Vogel, E. *Ab Initio* Potential Energy Curve for the Helium Atom Pair and Thermophysical Properties of the Dilute Helium Gas. II. Thermophysical Standard Values for Low-Density Helium. *Mol. Phys.* **2007**, *105*, 3035–3049.

(14) Klimeck, J.; Kleinrahm, R.; Wagner, W. An Accurate Single-Sinker Densimeter and Measurements of the (p,ρ,T) Relation of Argon and Nitrogen in the Temperature Range from (235 to 520) K at Pressures up to 30 MPa. *J. Chem. Thermodyn.* **1998**, *30* 1571–1588.

(15) Lösch, H. W.; Kleinrahm, R.; Wagner, W. Neue Magnetschwebewaagen für gravimetrische Messungen in der Verfahrenstechnik. Jahrbuch 1994, VDI-Gesellschaft Verfahrenstechnik und Chemieingenieurwesen (GVC); VDI-Verlag: Düsseldorf, 1994; pp 117−137.

(16) Kunz, O.; Klimeck, R.; Wagner, W.; Jaeschke, M. The GERG-2004 Wide-Range Equation of State for Natural Gases and Other Mixtures GERG TM15 2007. *Fortschr.-Ber. VDI, Reihe 6: Energietechnik*; VDI-Verlag: Düsseldorf, 2007; Nr. 557.

(17) Hendl, S.; Vogel, E. The Viscosity of Gaseous Ethane and Its Initial Density Dependence. *Fluid Phase Equilib.* **1992**, *76*, 259–272.

(18) Vogel, E. The Viscosity of Gaseous Propane and Its Initial Density Dependence. *Int. J. Thermophys.* **1995**, *16*, 1335–1351.

(19) Vogel, E.; Jäger, B.; Hellmann, R.; Bich, E. *Ab Initio* Pair Potential Energy Curve for the Argon Atom Pair and Thermophysical Properties for the Dilute Argon Gas. II. Thermophysical Properties for Low-Density Argon. *Mol. Phys.* **2010**, *108*, 3335–3352.

(20) Span, R.; Wagner, W. Equations of State for Technical Applications. II. Results for Nonpolar Fluids. *Int. J. Thermophys.* **2003**, *24*, 41–109.

(21) Funke, M.; Kleinrahm, R.; Wagner, W. Measurement and Correlation of the (p,ρ,T) Relation of Ethane. I. The Homogeneous

Gas and Liquid Regions in the Temperature Range from 95 K to 340 K at Pressures up to 12 MPa. *J. Chem. Thermodyn.* **2002**, *34*, 2001–2015.

(22) Funke, M.; Kleinrahm, R.; Wagner, W. Measurement and Correlation of the (*p*,*ρ*,*T*) Relation of Ethane. II. Saturated-Liquid and Saturated-Vapour Densities and Vapour Pressures along the Entire Coexistence Curve. *J. Chem. Thermodyn.* **2002**, *34*, 2017–2039.

(23) Claus, P.; Kleinrahm, R.; Wagner, W. Measurements of the (*p*,*ρ*,*T*) Relation of Ethylene, Ethane, and Sulphur Hexafluoride in the Temperature Range from 235 K to 520 K at Pressures up to 30 MPa Using an Accurate Single-Sinker Densimeter. *J. Chem. Thermodyn.* **2003**, *35*, 159–175.

(24) Claus, P.; Schilling, G.; Kleinrahm, R.; Wagner, W. *Internal Report*; Ruhr-Universität Bochum, 2002. Data were reported by Glos et al.[25]

(25) Glos, S.; Kleinrahm, R.; Wagner, W. Measurement of the (*p*,*ρ*,*T*) Relation of Propane, Propylene, *n*-Butane, and Isobutane in the Temperature Range from (95 to 340) K at Pressures up to 12 MPa Using an Accurate Two-Sinker Densimeter. *J. Chem. Thermodyn.* **2004**, *36*, 1037–1059.

(26) McLinden, M. O. Thermodynamic Properties of Propane. I. *p*-*ρ*-*T* Behavior from (265 to 500) K with Pressures to 36 MPa. *J. Chem. Eng. Data* **2009**, *54*, 3181–3191.

(27) Hendl, S.; Millat, J.; Vesovic, V.; Vogel, E.; Wakeham, W. A. The Viscosity and Thermal Conductivity of Ethane in the Limit of Zero Density. *Int. J. Thermophys.* **1991**, *12*, 999–1012.

(28) Kestin, J.; Leidenfrost, W. An Absolute Determination of the Viscosity of Eleven Gases over a Range of Pressures. *Physica* **1959**, *25*, 1033–1062.

(29) Kestin, J.; Paykoç, E.; Sengers, J. V. On the Density Expansion for Viscosity in Gases. *Physica* **1971**, *54*, 1–19.

(30) Kestin, J.; Ro, S. T.; Wakeham, W. A. Viscosity of the Noble Gases in the Temperature Range 25−700°C. *J. Chem. Phys.* **1972**, *56*, 4119–4124.

(31) Kestin, J.; Ro, S. T.; Wakeham, W. A. Reference Values of the Viscosity of Twelve Gases at 25°C. *Trans. Faraday Soc.* **1971**, *67*, 2308–2313.

(32) Kestin, J.; Khalifa, H. E.; Wakeham, W. A. The Viscosity of Five Gaseous Hydrocarbons. *J. Chem. Phys.* **1977**, *66*, 1132–1134.

(33) Abe, Y.; Kestin, J.; Khalifa, H. E.; Wakeham, W. A. The Viscosity and Diffusion Coefficients of the Mixtures of Four Light Hydrocarbon Gases. *Physica* **1978**, *93A*, 155–170.

(34) Iwasaki, H.; Takahashi, M. Viscosity of Carbon Dioxide and Ethane. *J. Chem. Phys.* **1981**, *74*, 1930–1943.

(35) Hunter, I. N.; Smith, E. B. Private Communication, Physical Chemistry Laboratory, Oxford, 1989.

(36) Vogel, E.; Küchenmeister, C.; Bich, E.; Laesecke, A. Reference Correlation of the Viscosity of Propane. *J. Phys. Chem. Ref. Data* **1998**, *27*, 947–970.

(37) Setzmann, U.; Wagner, W. A New Method for Optimizing the Structure of Thermodynamic Correlation Equations. *Int. J. Thermophys.* **1989**, *10*, 1103–1126.

(38) Younglove, B. A.; Ely, J. F. Thermophysical Properties of Fluids. II. Methane, Ethane, Propane, Isobutane, and Normal Butane. *J. Phys. Chem. Ref. Data* **1987**, *16*, 577–798.

(39) Abe, Y.; Kestin, J.; Khalifa, H. E.; Wakeham, W. A. The Viscosity and Diffusion Coefficients of the Mixtures of Light Hydrocarbons with Other Polyatomic Gases. *Ber. Bunsenges. Phys. Chem.* **1979**, *83*, 271–276.